I

0031-3998/98/4305-0683$03.00/0
PEDIATRIC RESEARCH

Vol. 43, No. 5, 1998
Printed in U.S.A.

Regional Distribution of Prostaglandin H Synthase-2 and Neuronal Nitric Oxide Synthase in Piglet Brain

RÓZSA DÉGI, FERENC BARI, TRACY C. BEASLEY, NISHADI THRIKAWALA, CLARA THORE, THOMAS M. LOUIS, AND DAVID W. BUSIJA

Departments of Ophthamology [R.D.] and Physiology [F.B.], Albert Szent-Györgyi Medical University, Szeged, Hungary; Department of Physiology and Pharmacology [T.C.B., N.T., C.T., D.W.B.], Bowman Gray School of Medicine of Wake Forest University, Winston-Salem, North Carolina 27157-1083; and Department of Anatomy and Cell Biology [T.M.L.], East Carolina University, School of Medicine, Greenville, North Carolina 27858-4353

ABSTRACT

Immunohistochemical techniques were used to examine the distribution of prostaglandin H synthase (PGHS)-2 and neuronal nitric oxide synthase (nNOS) in piglet brain. Samples from parietal cortex, hippocampus, and cerebellum were immersion fixed in 10% formalin, sectioned at 50 μm, and immunostained using specific antibodies against PGHS-2 and nNOS. Immunoreactivity for PGHS-2 was extensive throughout the areas examined. For example, PGHS-2 immunoreactive cells were present in all layers of the cortex, but were particularly dense among neurons in layers II/III, V, and VI. In addition, glial cells associated with microvessels in white matter showed PGHS-2 immunoreactivity. In contrast, nNOS immunoreactive neurons were limited in number and widely dispersed across all layers of the cortex and thus did not form a definable pattern. In the hippocampus, heavy PGHS-2 immunoreactivity was present in neurons and glial cells in the subgranular region, stratum radiatum, adjacent to the hippocampal sulcus, and in CA1 and CA3 pyramidal cells. Immunostaining for nNOS displayed a different pattern from PGHS-2 in the hippocampus, and was mainly localized to the granule cell layer of the dentate gyrus and the mossy fiber layer. In the cerebellum, PGHS-2 immunoreactivity was heavily represented in the Bergmann glia and to a lesser extent in cells of the granular layer, whereas nNOS was detected only in Basket cells. There are four conclusions from this study. First, PGHS-2 immunoreactivity is widely represented in the cerebral cortex, hippocampus, and cerebellum of neonatal pigs. Second, glia cells as well as neurons can show immunoreactivity for PGHS-2. And third, the distribution of nNOS is different from PGHS-2 immunoreactivity in the cerebral cortex, hippocampus, and cerebellum. (*Pediatr Res* **43: 683–689, 1998**)

Abbreviations

PGHS, prostaglandin H synthase
NOS, nitric oxide synthase
PGH_2, prostaglandin H_2
NO, nitric oxide
NGS, normal goat serum
GFAP, glial fibrillary acidic protein

PGHS (commonly called cyclooxygenase) converts membrane-linked arachidonic acid into an endoperoxide intermediate (PGH_2), which can be further converted into various prostaglandins and/or thromboxane (prostanoids) (1–3). PGHS exists in at least two isoforms, and these were originally and probably prematurely classified into constitutive (PGHS-1) and inducible (PGHS-2) varieties (1–4). Although both PGHS-1 and PGHS-2 have similar enzymatic actions, they have different molecular weights, exhibit different sensitivities to drugs such as indomethacin and dexamethasone, and have different distributions according to species, tissue, and experimental conditions (3–7). Although PGHS-1 is present under normal conditions in most cells, increasing evidence indicates that PGHS-2 is the predominant constitutive isoform in the neonate brains of several species. Thus, in piglet brain, mRNA for PGHS-2 is much more abundant than for PGHS-1, and vascular and cerebral prostaglandin production is largely inhibited by administration of a selective antagonist of PGHS-2 (6). Further, PGHS-2 immunoreactivity is more pronounced than that of PGHS-1 in large cerebral arteries of piglets (8). Similarly, PGHS-2 expression increases markedly during the third postnatal week in rats, after which levels return to a more limited, adult pattern (4).

The extent and distribution of PGHS-2 in the neonatal brain is an issue of particular interest for at least four reasons. First, prostanoids are an important component of cerebrovascular

Received November 17, 1997; accepted January 14, 1998
Correspondence: David W. Busija, Ph.D., Department of Physiology and Pharmacology, Bowman Gray School of Medicine, Medical Center Boulevard, Winston-Salem, NC 27157-1083.
Supported by National Institutes of Health Grants HL-30260, HL-46558, and HL-50587 and by the Hungarian Ministry of Education Grant FKFP 0713/1997.

control in neonatal animals and babies (9). Second, sick babies and/or pregnant women are often treated with drugs, such as indomethacin and dexamethasone, that differentially affect PGHS isoforms (1, 2). Third, metabolism of arachidonic acid by PGHS is the predominant pathway for the generation of superoxide anion in the cerebral cortex of piglets (10). And fourth, the location of PGHS may indicate a functional relationship to other bioactive substances, such as neuron-derived NO. However, the spatial relationships of PGHS-2 and nNOS in brain have not been examined.

The purpose of this study was to characterize the distributions of PGHS-2 and nNOS in the neonatal brain. We had several goals: first, to describe the pattern of PGHS-2 immunoreactivity in cerebral cortex, hippocampus, and cerebellum. These areas were chosen because they represent different stages of development in the neonatal brain (11), and because of their susceptibility to damage afer hypoxic/anoxic stress (12). Second, to characterize cellular location of PGHS-2 immunoreactivity within these areas. Although established astroglial populations in adult animals are usually negative for either PGHS isoform (13), the situation may be different for immature and radial astroglia in neonatal brains. For example, we find that cultured astroglia from the cerebral cortex of fetal lamb contain relatively large amounts of PGHS-2 (7). And third, to compare patterns of distribution of PGHS-2 with that of nNOS. Recent physiologic evidence suggests important functional interactions between the PGHS and NOS systems in the brain (11, 14–16), but the anatomical relationships which may underlie such interactions have not previously been investigated.

METHODS

All procedures were approved by the Animal Care and Use Committee at the Bowman Gray School of Medicine. Newborn pigs (1–5 d of age) were killed with an overdose of sodium thiopental. The brain was removed quickly, dissected according to region, and immersion fixed in 10% neutral, buffered formalin for 15–24 h. After washing in 10 mmol/L phosphate buffer containing 0.9% saline, pH 7.4 (PBS), 50-μm vibratome sections were cut and collected in 10 mmol/L PBS containing 0.1 mg/L thimerosal. All washes and solutions were made in PBS unless otherwise stated.

Immunohistochemistry. The sections were incubated in 50 mmol/L ammonium chloride for 1 h, washed, and incubated in 0.3% Triton X-100 for 1 h. After washing, the sections were blocked in 10% NGS/0.1% Tween 20 (NGS-T) for 4 h. Antibodies specific for PGHS-2 (Dr. A. W. Ford-Hutchinson, Merck Frosst Center for Therapeutic Research, Pointe Claire, CA; PG 26, Oxford, Oxford, MI) were diluted 1:2000 in NGS-T and incubated with sections overnight at room temperature. For consistency, all of the photomicrographs of the PGHS-2 immunostaining represent the antibody from Dr. Ford-Hutchinson. An antibody specific for human nNOS (Transduction Laboratories, Lexington, KY) was diluted 1:500 in NGS-T and incubated with sections overnight. After rinsing sections in NGS, endogenous peroxidase was blocked by incubating the sections in 3% H_2O_2/10% methanol for 30 min. After washing, anti-PGHS-2 sections were incubated for 2 h in biotinylated goat anti-rabbit IgG (Vector, Burlingame, CA), diluted 1:1000 in 2% NGS. Anti-nNOS sections were similarly treated and were incubated for 2 h in biotinylated goat anti-mouse IgG (Vector), which was diluted 1:1000 in 2% NGS for 2 h. Subsequently, sections were washed and reacted with Vector ABC reagent for 30 min, washed again, and reacted with diaminobenzidine. Stained sections were mounted on slides, dried, and cover slipped. Specificity of immunostaining was established using several approaches. Sections were incubated as described but without antibody (secondary antisera only) or with normal rabbit serum instead of primary antibody. In addition, anti-PGHS-2 was preadsorbed with 580 units of purified PGHS-2 (Cayman Chemical Co., Ann Arbor, MI) before incubation with sections.

Morphology. We used two approaches to characterize cellular patterns in the areas examined. First, general cellular morphology was assessed by cresyl violet staining. Second, immunostaining using an antibody (dilution 1:50,000) against GFAP was done using the same procedures as described above.

Figures. Sections were visualized and photographed with a Zeiss Axioskop microscope (Jena, Germany) and a Nikon camera. Figures were created with Adobe Photoshop software (San Jose, CA) from original 35-mm color slides and negatives, and were printed with a Fujix Pictograph 3000 digital printer (Encino, CA). Scanning contrast and intensity were altered only to replicate the original images. The digital images were converted to gray scale using filters as necessary, formatted to plate form, and labeled.

RESULTS

Parietal cortex. Immunolocalization of PGHS-2 in parietal cortex revealed widespread staining in all cortical laminae but was most pronounced in cortical layers II/III, V, and VI (Fig. 1*A*). Staining patterns for PGHS-2 were virtually identical using either antibody. Little or no cell specific immunoreactivity was observed when sections were incubated with secondary antibody only (Fig. 1*B*), normal rabbit serum instead of primary antibody (not shown), or PGHS-2 antibody which had been preadsorbed with purified PGHS-2 (not shown).

Cells of either oval shape (cortical layers II/III) or pyramidal shape (V) displayed characteristic perinuclear and somal PGHS-2 immunoreactivity with very little process staining (Fig. 1*D*). In fact, apical process staining for PGHS-2 was evident only in cells containing intense immunoreactivity. The variability in staining intensity of cells within a given region (cortical layers II/III are shown in Fig. 1*D*) was particularly evident at higher magnifications. Based on morphologic shape and the location and results of GFAP staining, the PGHS-2 immunoreactive cells within the cortical layers are most likely neurons.

In addition to the cortical staining, PGHS-2(+) cells were also present in white matter (Fig. 1, *A* and *E*). However, the pattern of PGHS-2 immunoreactivity in the white matter was quite different from that observed in the cortical layers (compare Fig. 1, *D* and *E*). Numerous small cells bearing PGHS-2 immunoreactive processes were observed. Often these posi-

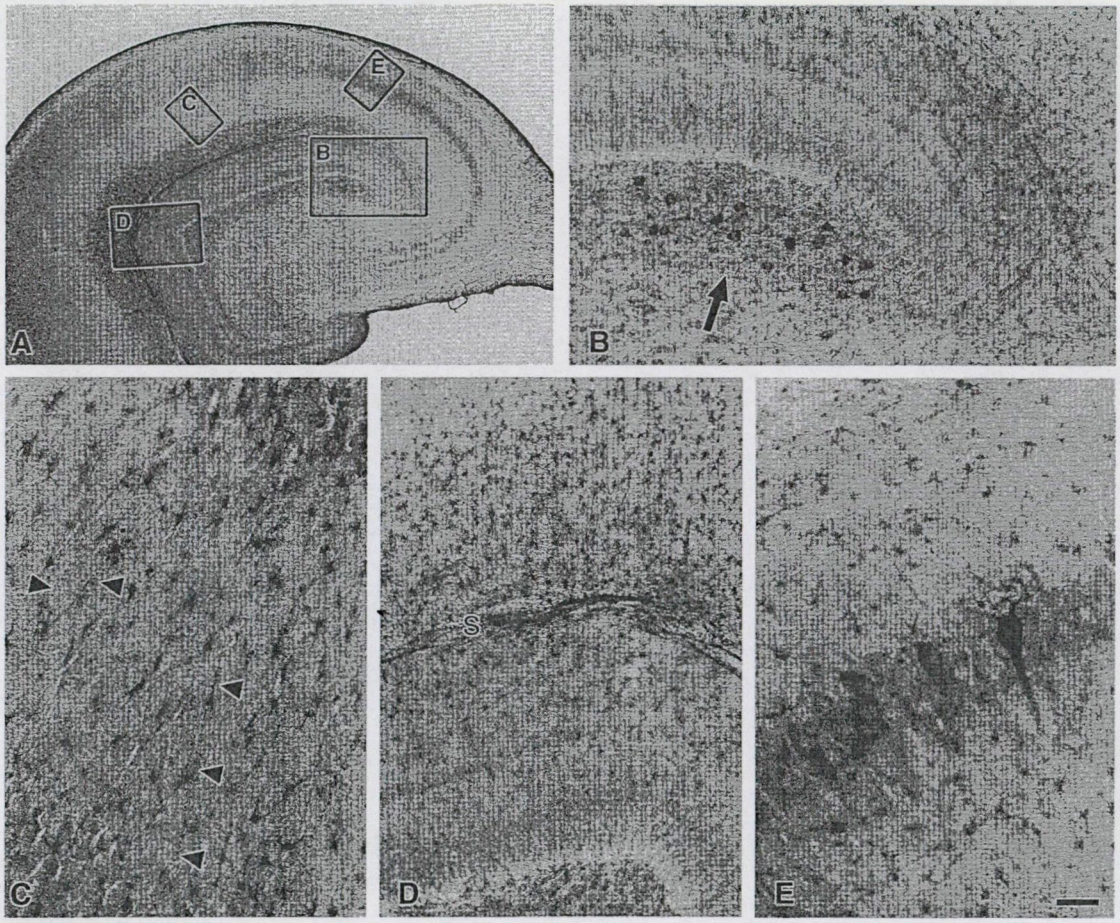

Figure 2. Immunolocalization of PGHS-2 in hippocampus. (*A*) Cross section of hippocampus showing anatomy of hippocampus and extensive PGHS-2 immunoreactivity. The boxed areas indicate the location of significant cell specific PGHS-2 reactivity in several areas, including (*B*) dentate gyrus, (*C*) stratum radiatum, (*D*) area adjacent to the hippocampal sulcus, and (*E*) CA3 pyramidal cells. These areas are shown at higher magnification in *panels B–E*. (*B*) PGHS-2 immunoreactivity was consistently observed in the soma of a group of neuron-like cells in the subgranular region located at the inner tip of the dentate gyrus. The *arrow* denotes an aggregate of these cells. (*C*) In the stratum radiatum, small, multipolar cells displayed immunoreactivity. Often processes were observed to contain areas of intense PGHS-2 staining (*arrowheads*). (*D*) Numerous small PGHS-2 staining cells were located along the hippocampal sulcus (*S*). (*E*) Pyramidal cells in CA3 displayed various intensities of PGHS-2 immunoreactivity. Scale bar = 1840 μm in *A*, 20 μm in *B*, 50 μm in *C*, 120 μm in *D*, and 25 μm in *E*.

cell layer and immediately inferior was a band of PGHS-2 immunoreactivity in the polymorphic layer of the dentate gyrus. Aggregates of large neurons located deep to the suprapyramidal blade consistently displayed relatively intense PGHS-2 immunoreactivity. The PGHS-2 staining of these cells appeared to localize in the cell bodies, surrounding the nucleus. In addition, the apical proximal portion of the processes of these cells also contained PGHS-2 immunoreactivity. Numerous small, star-shaped cells were located in the stratum radiatum (Fig. 2C) and in the molecular layers of the dentate and hippocampal gyri bordering the hippocampal fissure (Fig. 2*D*). The number of these small PGHS-2 positive cells appeared greater than in the adjacent stratum radiatum (compare Fig. 2, *C* and *D*) such that a prominent band of immunoreactivity was visible in the hippocampal and subicular molecular layers. In addition to the small cells in the stratum radiatum, PGHS-2 staining was seen in what are apparently axonal or glial processes (Fig. 2*C*, *arrowheads*). The pattern of GFAP immunoreactivity adjacent to the sulcus was very similar to the PGHS-2 staining of this region (not shown). Last, the pyramidal cells of the CA3 and CA1 fields and the subiculum displayed PGHS-2 immunoreactivity (Fig. 2*E*). The PGHS-2 immunoreactivity was very intense in the CA3 field, often extending into the hilar region. Although the PGHS-2 staining was fairly uniform in intensity, occasional neurons appeared darker than usual (Fig. 2*E*). Overall, PGHS-2 staining appeared to be present throughout the hippocampus and localized to both neurons and glial cells.

The hippocampus displayed a distinct staining pattern for nNOS (Fig. 3). Although scattered, intensely labeled cells were observed throughout the hippocampus, nNOS immunoreactivity was primarily localized to the granule cell layer of the dentate gyrus and the mossy fiber layer (Fig. 3*A*). Higher magnification of the suprapyramidal blade of the dentate gyrus region revealed perinuclear nNOS immunoreactivity in the granule cell layer and occasional immunoreactive cells in the polymorphic layer (Fig. 3*B*). However, unlike the PGHS-2 staining, a distinct aggregate of nNOS stained cells was never observed in the subgranular layer (compare Figs. 2*B* and 3*B*). In addition to the somal staining of the granular cells, their

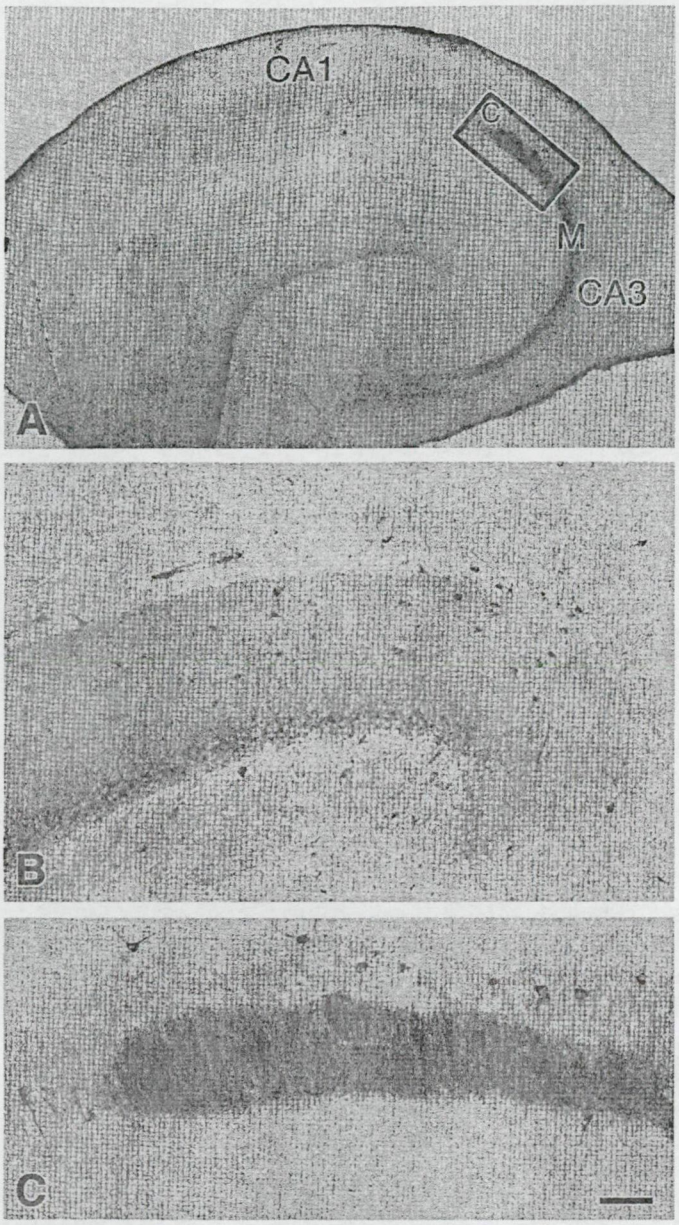

Figure 3. Immunolocalization of nNOS in hippocampus. (*A*) Representative cross-section of hippocampus showing pattern of nNOS immunoreactivity. Although occasional nNOS immunoreactive cells were observed throughout the hippocampus, the granular layer and mossy fiber layer (*M*) displayed the greatest staining. Very few cells were observed in the pyramidal cells in CA1 and CA3. (*B*) Higher magnification of the apical region of the dentate gyrus. Neuronal NOS immunoreactivity appears to be localized to the cell bodies of the granular cells. (*C*) Higher magnification of boxed area in *panel A*. Only occasional pyramidal and/or interneurons display nNOS immunoreactivity. However, the mossy fiber layer, which contains the axons of the granular cells, were consistently stained with nNOS. Scale bar = 1840 μm in *A*, 120 μm in *B*, and 368 μm in *C*.

axons, which comprise the mossy fiber layer, were also nNOS immunoreactive (Fig. 3*C*). Only an occasional pyramidal cell and/or interneuron in this region was stained for nNOS. Interestingly, the nNOS immunoreactive mossy fiber layer appeared adjacent to the CA3 pyramidal cells which are PGHS-2 positive (compare Figs. 2*E* and 3*C*). The distinct pattern of nNOS immunoreactivity appears to complement the PGHS-2 immunoreactivity in the dentate gyrus and CA3 pyramidal layer of the hippocampus.

Cerebellum. Immunostaining for PGHS-2 was present at various intensities in Purkinje cells and in the molecular and granular layers of the cerebellum (Fig. 4*A*). Like the parietal cortex and hippocampus, PGHS-2 immunoreactivity was detected in both neurons and glial cells. For example, a few cells in the granular layer were consistently observed and most likely represent neurons (Fig. 4*B*). Although the Purkinje cells themselves were never PGHS-2 positive, small cells adjacent to them were immunoreactive for PGHS-2 and GFAP. These small cells were probably Bergmann glia based upon double labeling against GFAP and PGHS-2. The thin processes that displayed PGHS-2/GFAP immunoreactivity in the molecular layer appear to be mostly the processes of the Bergmann glia, which are known to extend to the pial surface, but some could also represent processes of the granule cells (Fig. 4*B*).

The pattern of nNOS staining in the cerebellum differed greatly from that of PGHS-2 (compare Fig. 4, *B* and *C*). The only cells with detectable nNOS immunoreactivity were located in the molecular layer, adjacent to the Purkinje cell layer (Fig. 4*C*). Intense nNOS immunoreactivity was localized to the cell body and to the abundant processes of these cells. Based upon morphologic consideration, the nNOS stained cells in the molecular layer appear to be Basket cells.

DISCUSSION

There are several new findings from this study. First, PGHS-2 is widely represented in the cerebral cortex, hippocampus, and cerebellum of neonatal pigs. Second, glial cells as well as neurons can be immunoreactive for PGHS-2. And third, the distribution of nNOS differs from PGHS-2 in the cerebral cortex, hippocampus, and cerebellum. However, the spatial relationship between nNOS and PGHS-2 immunoreactivity is consistent with the hypothesis that these two systems can modify each other.

There is abundant evidence indicating that metabolites of PGHS play important roles in the regulation of the cerebral circulation and neural function. Basal and induced levels of prostanoids in cerebrospinal fluid in contact with cerebral arteries and arterioles are in the vasoactive range and are able to affect hemodynamics (9). Prostanoids also are involved in many brain functions, including those involving sleep, body temperature changes, and neuronal signaling (17–22).

Prostanoids appear to play a particularly important role in the regulation of the cerebral circulation during the perinatal period. In human babies, newborn pigs, and fetal lambs, inhibitors of PGHS reduce basal cerebral blood flow (9). In addition, in both babies and piglets, indomethacin treatment inhibits cerebrovascular dilator responses to arterial hypercapnia (9). Further, in piglets, PGHS products appear to participate in cerebrovascular responses to many stimuli (23, 24). In particular, prostanoids have potent and diverse effects on cerebrovascular responses to a number of neurotransmitters, including opioids, acetylcholine, oxytocin, norepinephrine, and kainate.

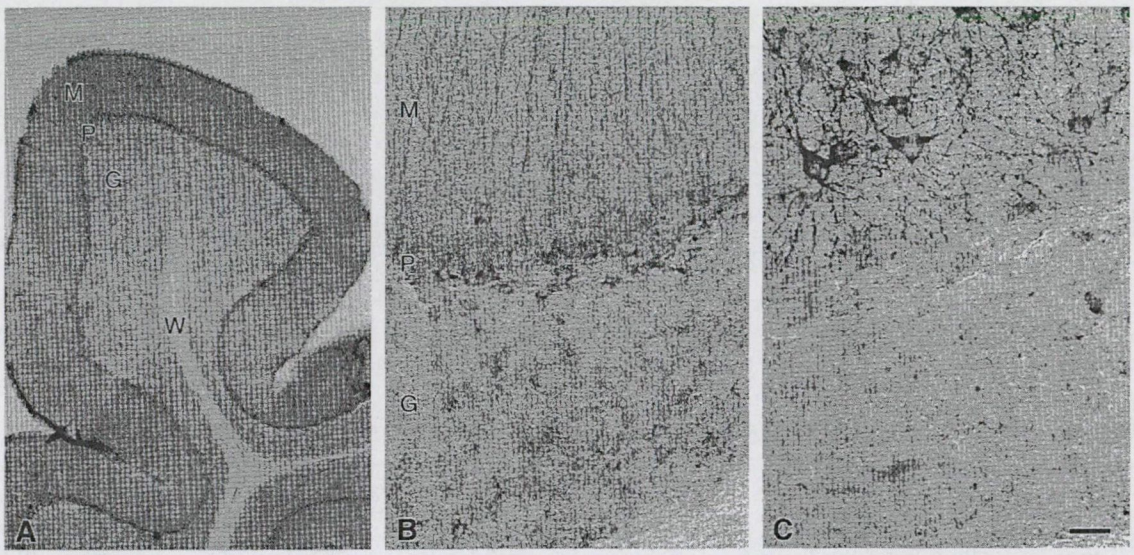

Figure 4. Immunolocalization of PGHS-2 and nNOS in cerebellum. (*A*) PGHS-2 immunoreactivity was observed in the molecular layer (*M*), Purkinje layer (*P*), and the granular layer (*G*). However, PGHS-2 staining was never detected in the white matter (*W*). (*B*) The most prominent PGHS-2 immunoreactivity was localized to small cells in the Purkinje cell layer. These cells are most likely Bergmann glia. Note that the Purkinje cells themselves do not appear to be stained for PGHS-2. Processes of the Bergmann glia in the molecular layer and occasional cells in the granular layer were also PGHS-2 positive. (*C*) The majority of nNOS immunoreactivity was localized to neuron-like cells, which may be basket cells, in the molecular layer. Like PGHS-2, the Purkinje cells lacked detectable nNOS immunoreactivity. Scale bar = 200 μm in *A*; 25 μm in *B* and *C*.

In addition to prostanoids, metabolism of arachidonic acid by PGHS also leads to the simultaneous production of superoxide anion. In particular, during reoxygenation after hypoxia or ischemia, relatively large amounts of superoxide anion are produced, and these radicals can alter neuronal and vascular function (11). Superoxide anion may act alone, or join together with NO to form peroxynitrite before inducing cell damage (14–15).

Only a few studies have examined localization of PGHS in brains of various species. In general, immunohistochemical studies indicate that PGHS isoforms are well represented in the brains of adult monkeys (25), sheep (13), and rats (4–5, 26). For example, PGHS-1 shows extensive immunostaining in the cerebral cortex and hippocampus of adult sheep and monkeys (13, 25). Our unpublished observations indicate little PGHS-1 immunoreactivity in these areas of the piglet brain, and confirm complementary data on mRNA and protein levels of PGHS isoforms in piglets (6).

Several lines of evidence support our immunohistochemical studies which indicate that PGHS-2 is the primary isoform in the neonatal brain. For example, mRNA for PGHS-2 is more prevalent in the piglet brain and cerebral circulation than PGHS-1 mRNA (6). Similarly, PGHS-2 protein abundance is greater than for PGHS-1 in most areas of the piglet brain and vasculature (6, 8). In addition, prostaglandin production in piglet cerebral tissues and vessels during arachidonic acid challenge is largely reduced by a selective PGHS-2 inhibitor (6). The current study extends these findings by documenting location and extent of PGHS-2. Thus, PGHS-2 immunoreactivity is extensively located in neurons and astroglia in cerebral cortex, hippocampus, and cerebellum. Similar to piglets, PGHS-2 appears to be particularly prominent in the neonatal rat (4). The reason for the predominance of PGHS-2 in the perinatal period is unclear, but it has been suggested to be due to augmented synaptic activity during development (4, 26, 27).

Immunostaining for PGHS-2 in piglet brains show several similarities and differences with that of adult rat. For example, the patterns of PHGS-2 immunostaining of neurons in cerebral cortex and hippocampus are similar in piglets and adult rats. Our demonstration of PGHS-2 immunostaining in axonal or glial processes in the stratum radiatum is similar to that reported by Kaufmann *et al.* (26). However, no PGHS-2 immunostaining was observed in the cerebellum of rats (5), whereas we found extensive positive staining of Bergmann glia and neurons in the granular layer in piglets. Additionally, we found substantial staining of glia cell populations in the cerebral cortex and hippocampus, whereas Breder *et al.* (5) found only neuronal staining.

Although particularly pronounced in neurons, significant PGHS-2 immunoreactivity was also present in specific populations of glial cells. Thus, astroglia associated with microvessels, particularly in the white matter of the cerebral cortex and hippocampus, and in Bergmann glia were immunopositive for PGHS-2. To our knowledge, ours is the first report of PGHS immunostaining of perivascular astrocytes. Although previous studies have indicated little or no PGHS-2 immunoreactivity in the cerebellum of a number of species, the Bergmann glia in piglets showed extensive immunostaining of cell bodies and processes. The pattern of staining that we observed was similar to that of PGHS-1 as reported by Smith *et al.* (28) for the adult pig, although the specificity of the antibody for this isoform is unclear. Thus, Bergmann glia, but not Purkinje cells, or cells in the molecular or granular layers were PGHS-1 positive in adult pigs. We did see diffuse staining for PGHS-2 in the granular cell layer. The difference in findings between neonatal and

adult pigs may be related to a conversion from PGHS-2 in the piglet to PGHS-1 as the animal matures (6, 26).

For the most part, nNOS showed patterns in cerebral cortex, hippocampus, and cerebellum that are distinct from PGHS-2. The low percentage of nNOS immunoreactive neurons observed in the piglet is similar to that reported in the cerebral cortex, hippocampus, and cerebellum of postnatal 7 d rats (29). In the cerebral cortex, nNOS immunostaining was relatively sparse but evenly distributed, whereas PGHS-2 immunoreactivity was extensive and particularly heavy in several layers. In the hippocampus, populations of cells immunopositive for nNOS or PGHS-2 were quite distinct, although overlap occurred in several areas such as the CA1/CA3. Finally, in the cerebellum nNOS and PGHS-2 were located in distinct cell populations. For example, Bergmann glia and neurons in the granular cell layer were PGHS-2 immunopositive, whereas basket cells were nNOS positive. The absence of significant nNOS immunoreactivity in Bergmann glia of piglets is different from that seen in other species (30).

The anatomical location of nNOS-containing cells is consistent with the possibility of NO modulating PGHS-2 function. Although there is apparently little overlap between nNOS and PGHS-2 immunoreactivity in specific cells or brain regions, nNOS neurons are located close enough to affect PGHS-2 containing cells in the cortex, hippocampus, and cerebellum. Although considered a relatively unstable compound, NO is able to diffuse across considerable distances in brain. For example, we have shown that activation of *N*-methyl-D-aspartic acid receptors, which are predominantly located in layers II/III of the piglet cortex (unpublished observations), cause NO-dependent dilation of pial arterioles that are approximately 200 μm away (31, 32). This distance places most nNOS-containing neurons close enough to affect PGHS-2-containing neurons and glial cells via release of NO.

Once released, there are at least two ways in which NO can modulate the PGHS system. First, NO may directly modulate activity of PGHS. Nitric oxide interacts with heme-containing compounds such as PGHS, and has been suggested to have variable effects on prostaglandin production or enzymatic activity (16, 33–35). The results of our recent study indicate that exogenous NO can suppress IL-induced increases in prostaglandin production by fetal ovine astroglia (16). Second, NO could combine with PGHS-dependent superoxide anion to form peroxynitrite (14, 15) which could damage adjacent cells.

In summary, PGHS-2 and nNOS have extensive distributions in neurons and glia in cerebral cortex, hippocampus and cerebellum. The spatial relationship between nNOS- and PGHS-2-immunopositive neurons and glial cells suggests that NO from the former could affect prostanoid production and promote peroxynitrite formation.

Acknowledgments. The authors thank Dr. A. W. Ford-Hutchinson of the Merck Frosst Center for Therapeutic Research, Pointe Claire, CA) for providing the PGHS-2 antibody, and Nancy Busija for editing the manuscript.

REFERENCES

1. DeWitt DL 1991 Prostaglandin endoperoxide synthase: regulation of enzyme expression. Biochim Biophys Acta 1083:121–134
2. Smith, WL 1992 Prostanoid biosynthesis and mechanisms of action. Am J Physiol 263:F181–F191
3. Wu KK 1996 Cyclooxygenase 2 induction: molecular mechanism and pathophysiologic roles. J Lab Clin Med 128:242–245
4. Yamagata K, Adreassson KT, Kaufmann WE, Barnes CA, Worley PF 1993 Expression of a mitogen-inducible cyclooxygenase in brain neurons: regulation by synaptic activity and glucocorticoids. Neuron 11:371–386
5. Breder CD, DeWitt D, Kraig RP 1995 Characterization of inducible cyclooxygenase in rat brain. J Comp Neurol 355:296–315
6. Peri KG, Hardy P, Li DY, Varma DR, Chemtob S 1995 Prostaglandin G/H synthase-2 is a major contributor of brain prostaglandins in the newborn. J Biol Chem 270:24615–24620
7. Thore CR, Nam MJ Busija DW 1996 Immunofluorescent localization of constitutive and inducible prostaglandin H synthase in ovine astroglia. J Comp Neurol 367:1–9
8. Busija DW, Thore C, Beasley T, Bari F 1996 Induction of cyclooxygenase-2 following anoxic stress in piglet cerebral arteries. Microcirculation 3:379–386
9. Busija DW 1997 Eicosanoids and cerebrovascular control. In: Welch KMA, Caplan LR, Reis DJ, Siesjö BK, Weir B (eds) Primer on Cerebrovascular Diseases. Academic Press, New York, pp 93–96
10. Pourcyrous M, Leffler CW, Bada HS, Korones SB, Busija DW 1993 Brain superoxide anion generation in asphyxiated piglets and the effect of indomethacin at therapeutic dose. Pediatr Res 34:366–369
11. Beasley TC, Bari F, Thore C, Thrikawala N, Louis TM, Busija DW 1998 Cerebral ischemia/reperfusion increases endothelial nitric oxide synthase levels via an indomethacin sensitive mechanism. J Cereb Blood Flow Metab, 18:88–96
12. Vannuci RC 1993 Mechanisms of perinatal hypoxic-ischemic brain damage. Semin Perinatol 17:330–337
13. Breder CD, Smith WL, Raz A, Masferrer J, Seibert K, Needleman P, Saper CB 1992 Distribution and characterization of cyclooxygenase immunoreactivity in the ovine brain. J Comp Neurol 322:409–438
14. Beckman JS, Beckman TW, Chen J, Marshall PA, Freeman BA 1990 Apparent hydroxyl radical production by peroxynitrite: implications for endothelial injury from nitric oxide and superoxide. Proc Natl Acad Sci USA 87:1620–1624
15. Beckman JS 1991 The double-edged role of nitric oxide in brain function and superoxide-mediated injury. J Dev Physiol 15:53–59
16. Busija DW, Thore C 1997 Modulation of prostaglandin production by nitric oxide in astroglia. Prostaglandins Leukot Essent Fatty Acids 56:355–359
17. Hedqvist P 1977 Basic mechanisms of prostaglandin action on autonomic neurotransmission. Annu Rev Pharmacol Toxicol 17:259–273
18. Ueno R, Narumiya S, Ogorochi T, Nakayama T, Ishikawa Y, Hayaishi O 1982 Role of prostaglandin D_2 in the hypothermia of rats caused by bacterial lipopolysaccharide. Proc Natl Acad Sci USA 79:6093–6097
19. Kimura H, Okamoto K, Sakai Y 1985 Modulatory effects of prostaglandins D_2, E_2 and $F_{2\alpha}$ on the postsynaptic actions of inhibitory and excitatory amino acids in cerebellar Purkinje cell dendrites *in vitro*. Brain Res 330:235–244
20. Stitt J 1986 Prostaglandin E as the neural mediator of the febrile response. Yale J Biol Med 59:137–149
21. Hayaishi O 1988 Sleep-wake regulation by prostaglandins D_2 and E_2. J Biol Chem 263:14593–14596
22. Shimizu T, Wolfe LS 1990 Arachidonic acid cascade and signal transduction. J Neurochem 55:1–15
23. Busija DW 1996 Nervous control of the cerebral circulation. In: T. Bennett and S. M. Gardiner (eds) Nervous Control of the Circulation. Harwood Academic Publishers, Amsterdam, pp 177–206
24. Bari F, Louis TM, Busija DW 1997 Kainate-induced cerebrovascular dilation is resistant to ischemia in piglets. Stroke 28:1272–1277
25. Tsubokura SY, Watanabe H, Ehara K, Imamura K, Saugimoto O, Kagamiyama H, Yamamoto S, Hayaishi O 1991 Localization of prostaglandin endoperoxide synthase in neurons and glia of the monkey brain. Brain Res 543:15–24
26. Kaufmann WE, Worley PF, Pegg J, Bremer M, Isakson P 1996 COX-2, a synaptically induced enzyme, is expressed by excitatory neurons at postsynaptic sites in rat cerebral cortex. Proc Natl Acad Sci USA 93:2317–2321
27. Adams J, Collaço-Moraes Y, de Belleroche J 1996 Cyclooxygenase-2 induction in cerebral cortex: an intracellular response to synaptic excitation. J Neurochem 66:6–13
28. Smith WL, Gutekunst DI, Lyons Jr RH 1980 Immunocytochemical localization of the prostaglandin-forming cyclooxygenase in the cerebellar cortex. Prostaglandins 19:61–69
29. Bredt DS, Synder, SH 1994 Transient nitric oxide synthase neurons in embryonic cerebral cortical plate, sensory ganglia, and olfactory epithelium. Neuron 13:301–313
30. Kugler P, Drenckhahn D 1996 Astrocyte and Bergmann glia as an important site of nitric oxide synthase I. Glia 16:165–173
31. Busija DW Leffler CW 1989 Dilator effects of amino acid neurotransmitters on piglet pial arterioles. Am J Physiol 257:H1200–H1203
32. Meng W, Tobin J, Busija DW 1995 Glutamate-induced cerebral vasodilation is mediated by nitric oxide through NMDA receptors. Stroke 26:857–863
33. Salvemini D, Misko TP, Masferrer JL, Seibert K, Currie MG, Needleman P 1993 Nitric oxide activates cyclooxygenase enzymes. Proc Natl Acad Sci USA 90:7240–7244
34. Stadler J, Harbrecht BG, DiSilivi M, Curran RD, Jordan ML, Simmons RL, Billiar TR 1993 Endogenous nitric oxide inhibits the synthesis of cyclooxygenase products and interleukin-6 by rat Kupffer cells. J Leuk Biol 53:165–172
35. Curtis JF, Reddy NG, Mason RP, Kalyanaraman B, Eling TE 1996 Nitric oxide: a prostaglandin H synthase 1 and 2 reducing cosubstrate that does not stimulate cyclooxygenase activity or prostaglandin H synthase expression in murine macrophages. Arch Biochem Biophys 335:369–376

II

ELSEVIER

Developmental Brain Research 107 (1998) 265–276

DEVELOPMENTAL BRAIN RESEARCH

Research report

Effects of anoxic stress on prostaglandin H synthase isoforms in piglet brain

Rózsa Dégi [a,c], Ferenc Bari [b,c], Nishadi Thrikawala [c], Tracy C. Beasley [c], Clara Thore [c], Thomas M. Louis [d], David W. Busija [c,*]

[a] *Department of Opthalmology, Albert Szent-Györgyi Medical University, Szeged, Hungary*
[b] *Department of Physiology, Albert Szent-Györgyi Medical University, Szeged, Hungary*
[c] *Department of Physiology and Pharmacology, Bowman Gray School of Medicine of Wake Forest University, Winston-Salem, NC 27157-1083, USA*
[d] *Department of Anatomy and Cell Biology, East Carolina University, School of Medicine, Greenville, NC 27858-4354, USA*

Accepted 13 January 1998

Abstract

We examined effects of ischemia and asphyxia on levels of prostaglandin H synthase-1 (PGHS-1) and prostaglandin H synthase-2 (PGHS-2) in piglet brain. Ischemia was induced by increasing intracranial pressure and asphyxia was induced by turning off the respirator. Duration of anoxic stress was 10 min. In some animals, indomethacin (5 mg/kg, i.v.) or 7-nitroindazole (7-NI) was administered prior to ischemia to block PGHS or brain nitric oxide synthase (bNOS), respectively. Tissues from cerebral cortex and hippocampus were removed and fixed and/or frozen after 1, 2, 4 and 8 h of recovery from anoxic stress. In addition, tissues were obtained from untreated animals or from time control animals. Levels of mRNA and proteins were determined using RNase protection assay and immunohistochemical approaches, respectively. In the tissues studied, only a few neurons were immunopositive for PGHS-1, and neither ischemia or asphyxia affected PGHS-1 immunostaining at 8 h after recovery. Likewise, PGHS-1 mRNA did not increase following anoxic stress. In contrast, substantial PGHS-2 immunoreactivity was present in neurons and glial cells in the cerebral cortex and hippocampus and there was no difference between time control and non treated animals. PGHS-2 mRNA increased by 2–4 h after ischemia, and heightened immunoreactivity for PGHS-2 was present at 8 h after ischemia in cerebral cortex and hippocampus. However, asphyxia did not increase PGHS-2 mRNA or immunostaining. Indomethacin pretreatment inhibited increases in mRNA and protein for PGHS-2 after ischemia, while 7-NI had little effect on increases in PGHS-2 immunoreactivity. We conclude that: (1) PGHS-2 is the predominant isoform present in piglet cerebral cortex and hippocampus; (2) Ischemia but not asphyxia increases levels of PGHS-2; (3) Ischemia does not increase levels of PGHS-1; and (4) Indomethacin but not 7-NI attenuates ischemia-induced increases in PGHS-2.

Keywords: Cyclooxygenase; Cerebral cortex; Hippocampus; Cerebellum; Ischemia; Asphyxia; Prostaglandin H synthase-1; Prostaglandin H synthase-2; Indomethacin; Nitric oxide synthase

1. Introduction

Hypoxia/ischemia is a relatively common occurrence in babies during the perinatal period. After successful resuscitation, hypoxia/ischemia is often followed 8–24 h later by secondary insults [37,38,40,41]. These insults, described in babies and experimental animals, include seizure activity, intracranial hemorrhages, edema, and secondary release of neurotransmitters such as glutamate. It is reasonable to speculate that changes in synthesis of specific proteins following the initial insult can predispose the brain to additional damage during these secondary insults.

One component of the original insult constituting anoxia/reoxygenation may be the damage caused by oxygen radicals. We and others have shown that the primary source of superoxide anion in the cerebral cortex in piglets and other species is through the metabolism of arachidonic acid by prostaglandin H synthase (PGHS; commonly referred to as cyclooxygenase) [2,32]. Superoxide anion is

* Corresponding author. Department of Physiology and Pharmacology, Bowman Gray School of Medicine, Medical Center Boulevard, Winston-Salem, NC 27157-1010, USA. Fax: +1-910-716-0237; E-mail: dbusija@bgsm.edu

0165-3806/98/$19.00
PII S0165-3806(98)00022-4

produced on a one-to-one basis with PGH_2, which is an unstable intermediate product that is further metabolized to various prostaglandins and/or thromboxanes (prostanoids). Further, we have shown that cerebrovascular dysfunction caused by transient anoxic stress can be prevented by administration of inhibitors of PGHS such as indomethacin or by administration of oxygen radical scavengers such as superoxide dismutase [4,5,12,24]. Further, nitric oxide (NO) is produced during ischemia/reperfusion [25] and potentially could combine with superoxide anion to form peroxynitrite [9].

Two isoforms of PGHS have been characterized [10,16,42,36]. Prostaglandin H synthase-1, appears to be the constitutive form in most tissues and organs excluding the brain and cerebral circulation. The inducible form (PGHS-2), is not normally widely represented in most tissues and organs except after cellular stress or damage. However, recent evidence indicates that PGHS-2 is constitutively present in the immature [10,30,31] as well as the mature brain [10]. Thus, in piglet brain, mRNA for PGHS-2 is more abundant than for PGHS-1, and prostaglandin production is primarily inhibited by administration of a selective antagonist of PGHS-2 [31]. Further, we have shown that PGHS-2 immunoreactivity is more pronounced than that of PGHS-1 in large cerebral arteries of piglets, and that vascular levels of PGHS-2 but not PGHS-1 increase rapidly after transient anoxic stress [13]. Increased PGHS-2 levels in cerebral arteries is associated with augmented capacity for prostacyclin production. A recent study has also shown that PGHS-2 levels increase in the adult rat brain following permanent cerebral ischemia. However, PGHS-2 levels are usually low and/or regionally localized in the normal, adult rat brain [10]. It is unclear whether levels of constitutively expressed PGHS-2 are increased in nonvascular tissues in the neonatal brain following anoxic stress. Augmented levels of PGHS isoforms in neurons and glial cells following anoxic stress might lead to enhanced capability for the production of superoxide anion during delayed, secondary insults, and thus promote additional neuronal injury.

The purpose of this study was to characterize effects of anoxic stress on brain levels of PGHS-1 and PGHS-2. We tested the hypothesis that anoxic stress would increase brain levels of PGHS-2 but not PGHS-1. We focused on responses in the cerebral cortex and hippocampus because these areas are particularly sensitive to anoxic stress in neonates [38]. In addition, we examined the effects of two different kinds of anoxic stress. Thus, piglets were exposed to 10 min of total global ischemia or 10 min of whole body asphyxia. We have shown previously that these interventions can have different effects on prostanoid- and non-prostanoid-dependent responses in the neonatal cerebral circulation [11]. Further, we examined effects of indomethacin pretreatment on increases in PGHS-2 following ischemia. Previous studies have shown that indomethacin pretreatment blocks superoxide anion production [2,3,32] and preserves cerebrovascular responsiveness [4,5,12,24] following cerebral ischemia. Finally, we examined effects of inhibition of brain nitric oxide synthase (bNOS) by 7-nitroindazole (7-NI) on increases in PGHS-2 following ischemia. Nitric oxide from bNOS has been suggested as a mediator of neuronal damage following ischemia [19,45], and the role of bNOS in regulating production of PGHS in brain has not been examined.

2. Materials and methods

All procedures were approved by the Animal Care and Use Committee at the Bowman Gray School of Medicine. Newborn (1–7 days old) pigs of either sex weighing between 0.9 and 1.4 kg were used. Anesthesia was induced with sodium thiopental (30–40 mg/kg, i.p.) followed by intravenous injection of α-chloralose (75 mg/kg). Supplemental doses of α-chloralose were given as needed to maintain a stable level of anesthesia. Animals were intubated by tracheotomy and artificially ventilated with room air. The ventilation rate (approximately 20 breaths/min) and tidal volume (approximately 20 ml/kg) were adjusted to maintain blood pH and gas values within physiological range. In our study, animals had baseline values within normal values for arterial pH (7.35–7.45), pCO_2 (30–35 mmHg), and pO_2 (80–100 mmHg).

Body temperature was maintained at 37–38°C by a water circulating heating pad. Systemic arterial blood pressure was recorded using a catheter placed into the right femoral artery connected to a pressure transducer. The right femoral vein was catheterized for administration of drugs and fluids and for withdrawal of blood. The head of the piglet was fixed in a stereotaxic frame. The scalp was incised and connective tissue over the parietal bone was removed. A craniotomy for a stainless steel–glass cranial window 19 mm in diameter was made in the left parietal bone approximately 10 mm rostral to the coronal suture. The dura was exposed, cut and reflected over the skull. A cranial window with three needle ports was placed into the craniotomy, sealed with bone wax and cemented with SuperGlue® (Atlanta, GA) and dental acrylic. The closed window was filled with artificial cerebrospinal fluid (aCSF) warmed to 37°C and equilibrated with 6% O_2 and 6.5% CO_2 in N_2. The aCSF consisted of: KCl 2.9, $MgCl_2$ 1.4, $CaCl_2$ 1.2, NaCl 132, $NaHCO_3$ 24.6, urea 6.7 and glucose 3.7 mmol/l. Blood flow through pial arterioles was observed using a microscope (Wild M36, Heerbrugg, Switzerland) equipped with a video camera (Panasonic, Secaucus, NJ).

Anesthetized, instrumented piglets were divided into three groups: asphyxia ($n = 12$), ischemia ($n = 21$), and time control ($n = 17$). Some animals received indomethacin (5 mg/kg, i.v.) ($n = 7$) or 7-NI (50 mg/kg, i.p.) ($n = 12$) prior to ischemia. Indomethacin is an effective blocker of PGHS in cerebral tissues of piglets

[2,4,5,11,24,32]. In addition, 7-NI is an effective blocker of bNOS in piglets [6]. Asphyxia was achieved by turning off the ventilator and clamping the endotracheal tube, as described previously [11,13,32]. After 10 min of asphyxia, the tubing was unclamped and the animals were reventilated. During asphyxia, intravenous epinephrine was given as needed to prevent asystole and during reventilation, 3 ml/kg of a 4.2% $NaHCO_3$ solution was given to counteract systemic acidosis. Cerebral ischemia-reperfusion injury was produced as described previously [5,24]. To summarize, a hollow brass bolt was placed in the left cranium without damaging the dura. The bolt allowed infusion of aCSF into the cranium resulting in an increase in intracranial pressure. Venous blood was withdrawn as necessary to maintain mean arterial pressure within normal values. A complete cessation of blood flow to the cortex was evaluated by intravital microscopy. Microsphere experiments indicate that blood flow to the entire brain becomes undetectable during increased intracranial pressure [8]. After 10 min of ischemia, the infusion tube was clamped and the intracranial pressure was allowed to normalize. Time control animals were treated like the other two groups but were not exposed to asphyxia or ischemia. Animals were killed while anesthetized with intravenous KCl at 1, 2, 4, 6, and/or 8 h after ischemia or asphyxia, and the brains removed. In addition, several non-treated animals ($n = 6$) were killed with an overdose of sodium thiopental (150 mg/kg, i.p.), and their brains removed.

The brain was removed quickly and samples of cerebral cortex and hippocampus were immersion fixed in 10%

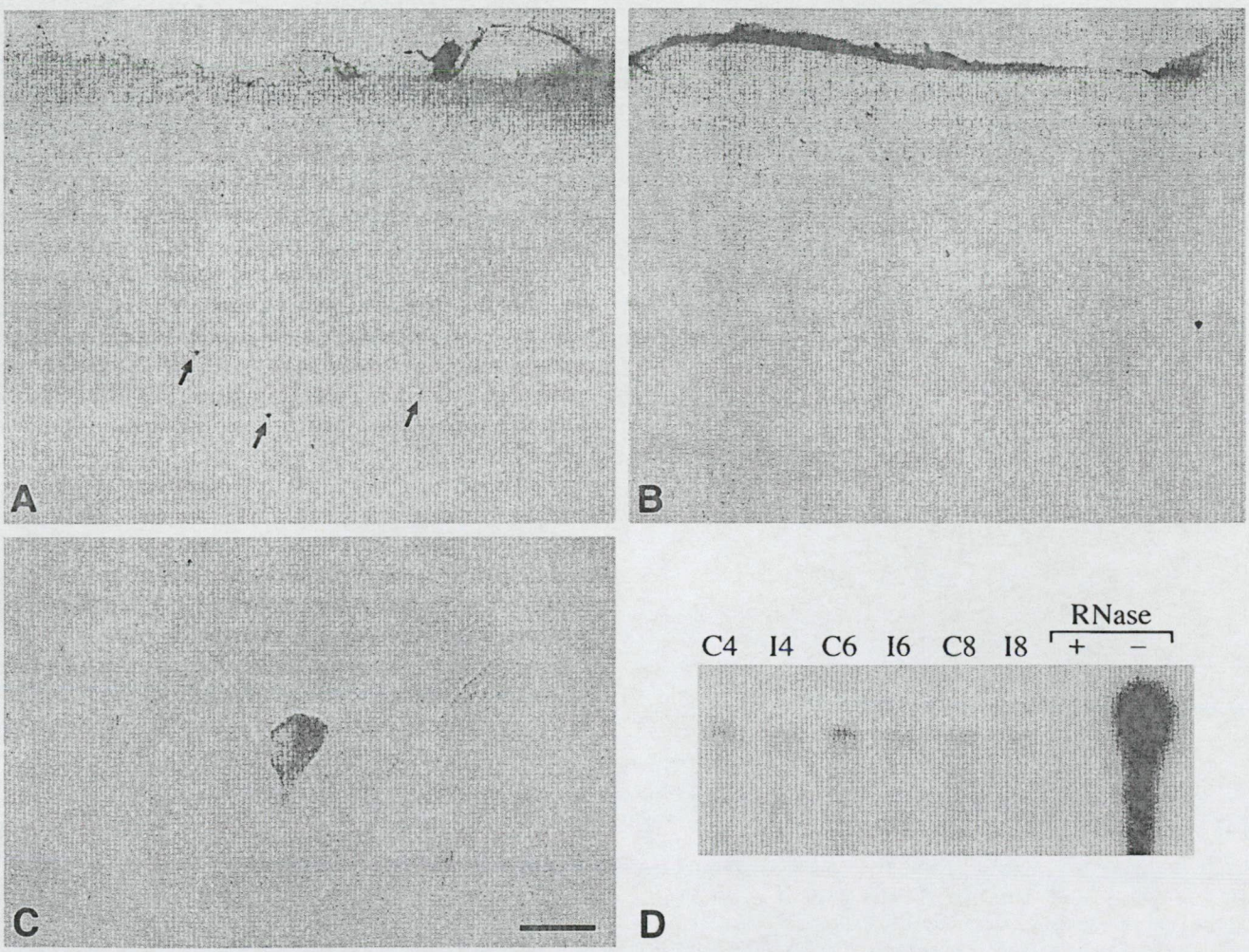

Fig. 1. PGHS-1 representation in cerebral cortex. (A) Only a few neurons (arrows) were immunopositive for PGHS-1 in a 8 h time control animal. (B) No significant increase in PGHS-1 immunoreactivity was detected in cortex 8 h after ischemia. (C) Higher magnification of one of the neurons shown in A. PGHS-1 immunoreactivity was localized to the cell body with no immunostaining extending into the processes. (D) RNase Protection Assay showed detectable PGHS-1 mRNA in time control animals, but no increase in mRNA following ischemia. Long X-ray exposure times relative to those for PGHS-2 blots (see Fig. 2) were necessary to detect PGHS-1 mRNA in piglet cortex. The 4, 6, and 8 h time control lanes are indicated as C4, C6, and C8, respectively. Likewise, 4, 6, and 8 h after ischemia are indicated as I4, I6, and I8, respectively. Unprotected probe digested with RNase is shown in '+' lane, while the unhybridized, undigested probe is shown in the '−' lane. Note that the unprotected band shown in the last lane of the blots runs at 293 bp and the hybridized bands migrate at 235 bp. Bar represents 200 μm in panels A and B and 25 μm in panel C.

neutral, buffered formalin for 15–24 h or frozen by immersion in 2-methyl butane at −70°C. Frozen samples were stored at −60°C. In addition, samples from cerebellum, thalamus, and superior colliculus were frozen.

2.1. Immunohistochemistry

After washing in 10 mmol/l phosphate buffer containing 0.9% saline, pH 7.4 (PBS), 50 μm vibratome sections were cut and collected in 10 mmol/l PBS containing 0.1 mg/l of thimerosal. All washes and solutions were made in PBS unless otherwise stated. The sections were incubated in 50 mmol/l ammonium chloride for an hour, washed, and incubated in 0.3% Triton X-100 for another hour. After washing, the sections were blocked in 10% normal goat serum (NGS)/0.1% tween 20 (NGS-T) for 4 h. Antibodies specific for PGHS-1 (Dr. Steve Prescott, Salt Lake City, UT) and PGHS-2 (Dr. A.W. Ford-Hutchinson, Merck Frosst Center for Therapeutic Research, Pointe Claire, Quebec, Canada or PG 26, Oxford, Oxford, MI) were diluted 1:2000 and 1:10,000, respectively, in NGS-T and incubated with brain sections overnight at room temperature. The use of either PGHS-2 antibody yielded virtually identical results. For consistency, all of the photomicrographs of PGHS-2 immunostaining represent the use of the antibody from Dr. Ford-Hutchinson. After rinsing sections in NGS, endogenous peroxidase was blocked by incubating the sections in 3% H_2O_2/10% methanol for 30 min. After washing, anti-PGHS-2 sections were incubated for 2 h in biotinylated goat anti-rabbit IgG (Vector, Burlingame, CA), diluted 1:1000 in 2% NGS. Anti-PGHS-1 sections were similarly treated and were incubated for 2 h in biotinylated goat anti-mouse IgG (Vector), which was diluted 1:1000 in 2% NGS for 2 h. Subsequently, sections were washed and reacted with Vector ABC reagent (Vector) for 30 min, washed again, and reacted with diaminobenzidine. Stained sections were mounted on slides, dried, and coverslipped. Specificity of immunostaining was established using several approaches. Sections were incubated as described but without antibody (secondary antisera only) or with normal rabbit serum instead of primary antibody. In addition, the PGHS-2 antibody was preadsorbed with 580 units of purified PGHS-2 (Cayman Chemical, Ann Arbor, MI) prior to incubation with sections.

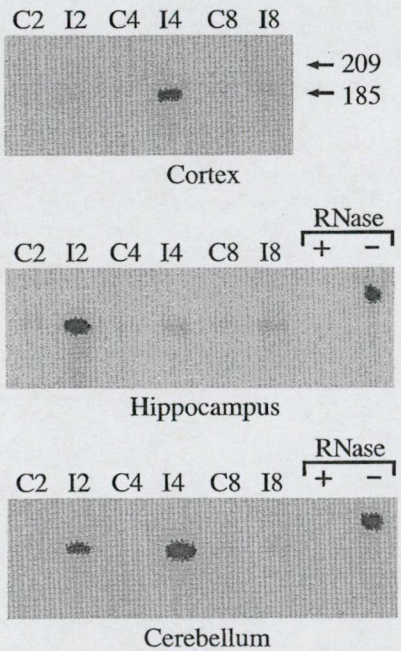

Fig. 2. Upregulation of PGHS-2 mRNA after global cerebral ischemia. RNase Protection Assay revealed increased expression of PGHS-2 mRNA at 2–4 h in cerebral cortex, hippocampus, and cerebellum. The 2, 4, and 8 h time control lanes are indicated as C2, C4, and C8, respectively. Likewise, 2, 4, and 8 h after ischemia are indicated as I2, I4, and I8, respectively. Unprotected probe digested with RNase is shown in '+' lane, while the unhybridized, undigested probe is shown in the '−' lane. Lane labels for the hippocampus and cerebellum blots are identical to those of the cortex. Note that the unprotected band shown in the last lane of the hippocampus and cerebellum blots runs at 209 bp and the hybridized bands migrate at 185 bp.

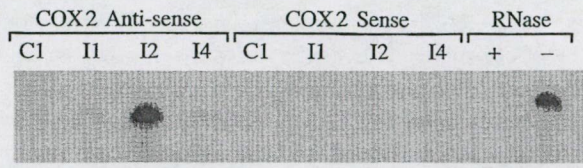

Fig. 3. Comparison of bands of protected fragments of PGHS-2 mRNA from hippocampus run with anti-sense and sense probes. RNA samples used with anti-sense and sense probes are aliquots from the same stock. The sense probe did not detect mRNA. Lanes as labeled in Fig. 2.

We used two approaches to characterize cellular patterns in the areas examined. First, general cellular morphology was assessed by cresyl violet staining. Second, immunostaining using an antibody (dilution 1:50,000) against glial fibrillary acidic protein (GFAP) was done using the same procedures as described above.

Sections were visualized and photographed with a Zeiss Axioskop microscope (Jena, Germany). Figures were created with Adobe Photoshop (San Jose, CA) software from

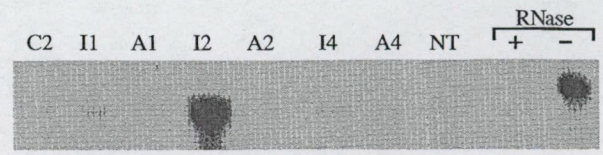

Fig. 4. Comparison of the effects of global cerebral ischemia and whole body asphyxia on PGHS-2 mRNA in hippocampus. A transient increase in PGHS-2 mRNA occurred after cerebral ischemia while no change was detected within 4 h after asphyxia. Note that there is also very little difference between the 2 h time control band (C2) and the untreated band (NT). The ischemia lanes are indicated by 'I' and asphyxia lanes are indicated by 'A'. The numbers refer to the time after anoxic stress. The PGHS-2 probe lanes are as marked in Fig. 2.

original 35 mm color slides and negatives and were printed with a Fujix Pictograph 3000 digital printer (Encino, CA). Scanning contrast and intensity were altered only in order to replicate the original images. The color images were converted to gray scale using filters as necessary, formatted to plate form, and labeled.

2.2. RNase protection assay (RPA)

Total RNA was extracted in homogenization buffer (4 M guanidium isocyanate, 25 mM/l sodium acetate, 0.1 M/l β-mercaptoethanol). After sonication, the homogenates were transferred to phase lock gel tubes (5-

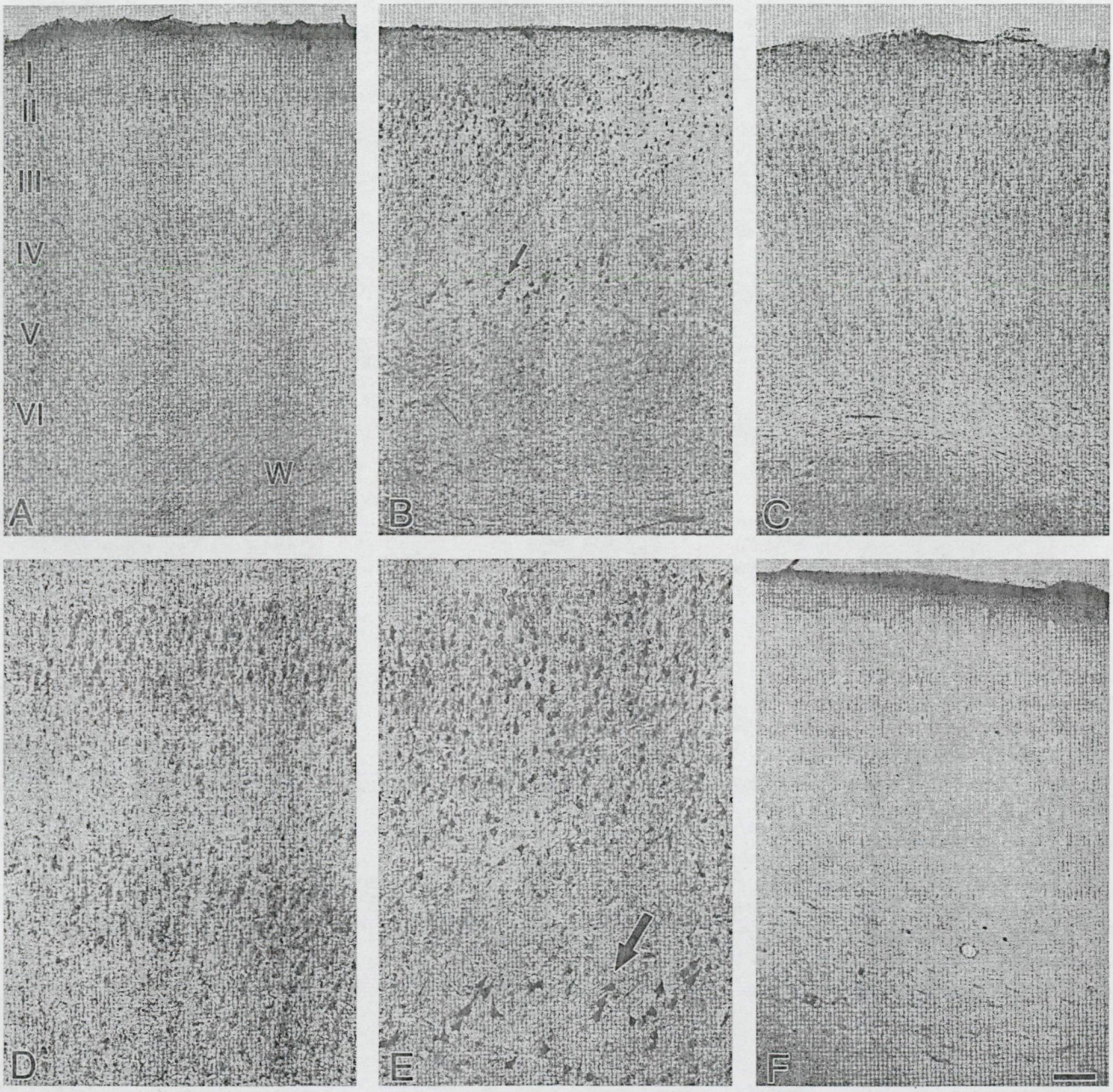

Fig. 5. Effect of anoxic stress on PGHS-2 immunoreactivity in 50 μm sections from cerebral cortex. (A) Parietal cortex from 8 h sham time control piglet showing uniform PGHS-2 staining primarily in cortical layers II/III, V, and VI. Some staining of smaller cells can be observed in the white matter (W). Roman numerals indicate cortical layers. (B) PGHS-2 immunoreactivity was increased 8 h after global cerebral ischemia in cortical layers II/III, V and VI. Arrow indicates characteristic neuron which can be seen at higher magnification in panel E. (C) Asphyxia did not appear to alter the intensity or pattern of PGHS-2 staining in parietal cortex. (D) Higher magnification of time control parietal cortex shown in panel A. (E) Higher magnification of ischemia parietal cortex shown in panel B. (F) PGHS-2 immunoreactivity following preadsorption of primary antibody with PGHS-2. Scale bar = 200 μm in A, B, and C. 120 μm in D, E, and F.

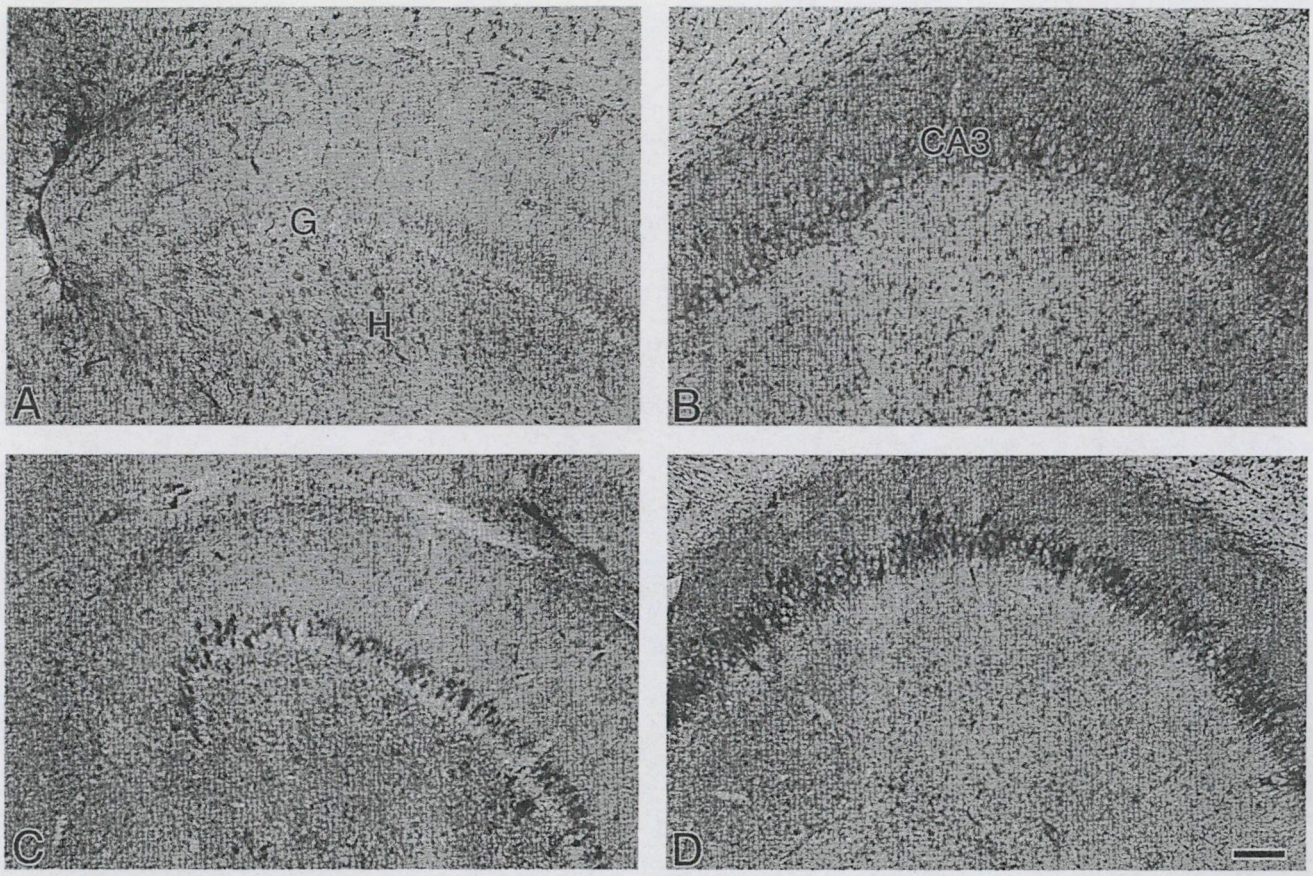

Fig. 6. Immunolocalization of PGHS-2 in 50 μm sections from hippocampus after anoxic stress. (A) Suprapyramidal blade of the dentate gyrus from a time control piglet. PGHS-2 immunoreactivity was consistently observed in a distinct patch of neurons in the polymorphic layer of this area. (B) The CA3 pyramidal layer of time control piglets had modest to low levels of PGHS-2 immunoreactivity. (C) At 8 h after global cerebral ischemia, PGHS-2 immunoreactivity was observed in the granule layer of the dentate gyrus. Concomitantly, there was a decrease in PGHS-2 staining of the polymorphic neurons in this region. (D) An increase in PGHS-2 immunostaining of filed CA3 neurons occurred after global cerebral ischemia. Scale bar = 120 μm.

prime-3-prime, Boulder, CO). Then, 100 μl of 2 M/l sodium acetate was added to each sample, followed by addition of 1 ml of H_2O-saturated phenol. After thorough mixing, 300 μl of chloroform:isoamyl alcohol (49:1) was added, and the solution was incubated on ice for 10 min before centrifugation at 6000 rpm for 5 min. The supernatants were transferred to fresh tubes. After adding 1 ml of isopropanol, the samples were incubated in room temperature for 30 min and centrifuged at 12,000 rpm for 25 min. The resulting pellets were washed with 100% ethanol and redissolved in ultra pure water before storing in −60°C. The integrity of RNA was determined by resolving in a 1% agarose gel and RNA aliquots were quantified using a spectrophotometer.

Ribonuclease protection assays were done on 25 μg of total RNA from each sample using RPA II kits (Ambion, Austin, TX). ^{32}P-labeled sense and antisense probes were generated for PGHS-1 and PGHS-2 using MaxiScript kits (Ambion) after linearizing plasmids containing fragments of DNA for porcine PGHS-1 and -2 (Dr. Sylvain Chemtob, Research Centre of St. Justine Hospital, Montreal, Canada). The protected fragments were resolved on 6% urea/acrylamide gel and autoradiographed using hyperfilm (Amersham, Arlington Heights, IL).

3. Results

3.1. PGHS-1

Very little immunoreactivity for PGHS-1 was present in cerebral cortex (Fig. 1A,C) or hippocampus (not shown) from samples taken from time control or non-treated ani-

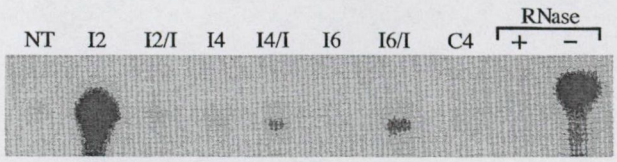

Fig. 7. Effects of indomethacin pretreatment (5 mg/kg, i.v.) on PGHS-2 mRNA in hippocampus following ischemia. Indomethacin pretreatment (/I) attenuated the large increase in mRNA normally seen early after ischemia. Lane designations are the same as used in Figs. 2–4.

mals. In addition, mRNA for PGHS-1, while detectable, was relatively low in time control animals (Fig. 1D). Detection of mRNA for PGHS-1 required longer incubation times of gels with film than for PGHS-2 (compare sample versus probe lanes for PGHS-1 in Fig. 1D with PGHS-2 in Figs. 2–4 and 7). Further, immunoreactivity (Fig. 1B) or mRNA levels (Fig. 1D) for PGHS-1 did not increase following anoxic stress in any region examined.

3.2. PGHS-2

3.2.1. RNase protection assay

Global cerebral ischemia transiently increased the expression of PGHS-2 mRNA in parietal cortex and hippocampus (Figs. 2–4). In cerebral cortex, upregulation of PGHS-2 mRNA was variable and occurred at 2–4 h and returned to control levels by 8 h (Fig. 2 top; Fig. 3). For

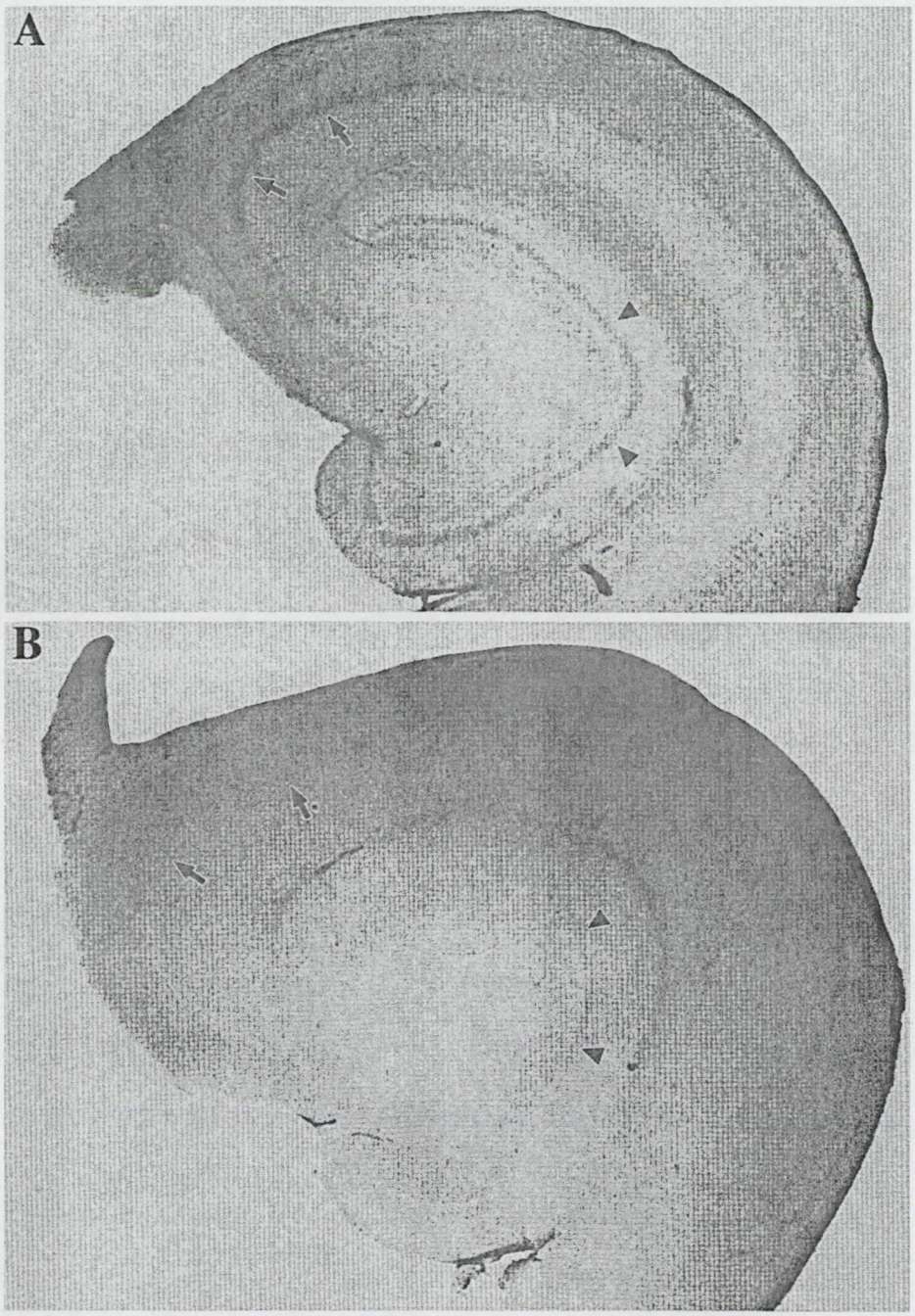

Fig. 8. Effects of indomethacin pretreatment (5 mg/kg, i.v.) on immunolocalization for PGHS-2 8 h after ischemia on 50 μm sections from hippocampus. (A) Ischemia increased PGHS-2 immunostaining in field CA3 neurons (arrows) and in the polymorphic layer of the dentate gyrus (points). (B) Indomethacin pretreatment completely eliminated increased immunostaining for PGHS-2 in these areas. Original magnification is 3.91 × for A and 3.125 × for B.

cortex, we converted the density of bands into pixels using the NIH Image Analysis software (version 1.55). Density values of mRNA for cortex were 886 ± 234 pixels (mean ± standard error) for time control animals ($n = 16$), 3430 ± 2136 pixels for animals 2 h after ischemia ($n = 7$), 5257 ± 1319 pixels for animals 4 h after ischemia ($n = 8$), and 1385 ± 33 pixels for animals 8 h after ischemia ($n = 2$) ($P < 0.05$, time control version 4 h ischemia animals). For hippocampus, increased PGHS-2 mRNA levels occurred consistently at 2 h after ischemia (Fig. 2middle; Fig. 4). Further, PGHS-2 mRNA remained only slightly increased over control levels at 4 and 8 h after ischemia in hip-

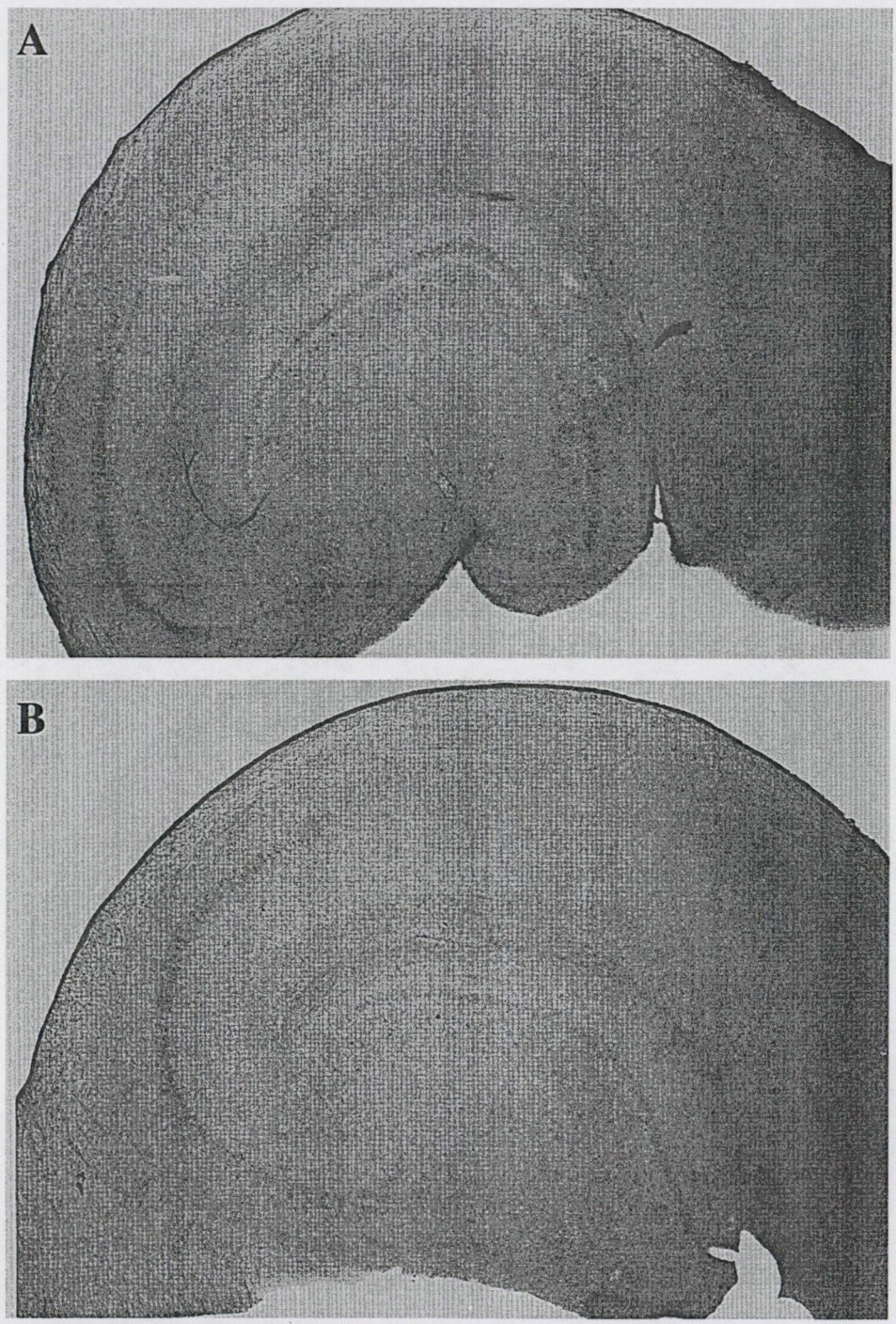

Fig. 9. Effects of 7-NI on immunolocalization for PGHS-2 8 h after ischemia on 50 μm sections from hippocampus. (A) Ischemia alone. (B) Ischemia following pretreatment with 7-NI (50 mg/kg, i.p. given before ischemia, and also 4 h after ischemia). There was no consistent effect of 7-NI treatment on increases in PGHS-2 immunoreactivity after ischemia. Original magnification is 3.125 × for both A and B.

pocampus. Increases in mRNA for PGHS-2 occurred in other areas of the brain within 2-4 h after ischemia, for example, in cerebellum (Fig. 2 bottom) and in superior colliculus and thalamus (not shown). Use of the sense probe for PGHS-2 failed to produce bands on the gel (Fig. 3).

In contrast to ischemia, asphyxia did not appear to alter PGHS-2 mRNA levels throughout the 8 h reoxygenation period in hippocampus (Fig. 4) or in cerebral cortex or cerebellum (not shown). Thus, increased PGHS-2 mRNA synthesis appeared to be sensitive to the mode of anoxic stress employed.

3.2.2. *Immunohistochemistry*

3.2.2.1. Cerebral cortex. Immunolocalization of PGHS-2 in cerebral cortex from 8 h time control piglets revealed widespread staining in virtually all cortical layers, but immunoreactivity was readily evident in layers II/III, V, and VI (Fig. 5A,D). The PGHS-2 immunoreactivity throughout the layers was moderate and uniform in intensity and was most evident in pyramidal neurons of layer V (Fig. 5D). Little or no cell specific immunoreactivity was observed when sections were incubated with secondary antibody only, normal rabbit serum instead of primary antibody, or PGHS-2 antibody which had been preadsorbed with purified PGHS-2 (Fig. 5F). The pattern of PGHS-2 immunoreactivity in the parietal cortex from time control animals was nearly identical to that taken from untreated animals (not shown).

Global cerebral ischemia increased the intensity of PGHS-2 immunoreactivity in parietal cortex (Fig. 5 compare B to A). The increase in PGHS-2 immunoreactivity occurred primarily in cortical layers which contained basal PGHS-2 staining (i.e., II/III, V, and VI). At higher magnification, the perinuclear staining of pyramidal neurons could be observed within cortical layers II/III and V (Fig. 5D [time control], E [ischemia]). PGHS-2 immunoreactivity was also evident in the proximal portion of the apical processes of intensely stained neurons (Fig. 5E). Unlike ischemia, whole body asphyxia did not appear to alter the pattern or intensity of PGHS-2 immunoreactivity in parietal cortex (Fig. 5C).

3.2.2.2. Hippocampus. While PGHS-2 immunoreactivity was evident in various regions, an aggregate of subgranular, polymorphic neurons in the superficial hilus of the dentate gyrus consistently displayed intense immunostaining in time control samples (Fig. 6A). Limited PGHS-2 immunoreactivity was also observed in field CA3 pyramidal cells (Fig. 6B), although the intensity was more variable than that detected in the dentate gyrus. Uniform and widespread PGHS-2 immunoreactivity was also observed in small stellate cells in the molecular layer of the hippocampus and bordering the hippocampal fissure (Fig. 6A,B). The pattern of PGHS-2 staining in time control animals was virtually identical to that of untreated piglets (not shown).

Global cerebral ischemia altered the pattern of PGHS-2 immunoreactivity primarily in the polymorphic and granule layers of the dentate gyrus and in field CA3 of Ammon's horn. By 8 h after ischemia, virtually no subgranular neurons in the polymorphic layer of the dentate were immunoreactive for PGHS-2 (Fig. 6C). Instead, intense PGHS-2 immunoreactivity was localized to cells within the granule layer of the dentate gyrus (Fig. 6C). Further, the intensity of PGHS-2 immunoreactivity in the pyramidal neurons in CA3 was greater and more consistent than in time controls (Fig. 6B,D). While PGHS-2 immunoreactivity was greatly increased in both the dentate granule and CA3 pyramidal layers, no detectable changes were observed in the staining of the small stellate cells bordering the hippocampus. Unlike ischemia/reperfusion injury, no detectable changes in either the pattern or the intensity of PGHS-2 immunostaining were observed after whole body asphyxia (not shown). Thus, global cerebral ischemia increased not only the intensity of staining in pyramidal cells of Ammon's horn but also augmented PGHS-2 immunostaining in the granule cells of the dentate gyrus.

3.2.2.3. Indomethacin treatment. Systemic pretreatment with indomethacin prevented increases in PGHS-2 mRNA at 2 h after ischemia (Fig. 7). In addition, indomethacin pretreatment prevented increases in PGHS-2 immunoreactivity at 8 h after ischemia in hippocampus (Fig. 8) and cerebral cortex (not shown).

3.3. *7-NI treatment*

Systemic pretreatment with 7-NI did not prevent increases in mRNA for PGHS-2 (not shown) following ischemia. Further, 7-NI pretreatment had no substantial, consistent effect on increases in PGHS-2 immunoreactivity at 8 h after ischemia in hippocampus (Fig. 9) and cerebral cortex (not shown).

4. Discussion

The major findings were: (1) PGHS-2 is the predominant isoform in piglet brain; (2) PGHS-2 but not PGHS-1 mRNA and protein levels increase following ischemia; (3) PGHS-2 mRNA and protein levels fail to increase after asphyxia; (4) Indomethacin pretreatment attenuates increases in PGHS-2 mRNA and protein levels after ischemia; and (5) 7-NI pretreatment has little effect on increases in PGHS-2 levels after ischemia. These results demonstrate that PGHS-2 levels are differentially affected by the type of anoxic stress, and that increases in PGHS-2 after ischemia are dependent on indomethacin—but not 7-NI-sensitive mechanisms.

Our current findings confirm previous studies by our laboratory [13,15] and others [30,31] which indicate that PGHS-2 is the predominant isoform in the neonatal pig. For example, mRNA for PGHS-2 is more abundant in the piglet brain and cerebral circulation than PGHS-1 mRNA [31]. In addition, PGHS-2 protein is predominant over PGHS-1 levels in most brain areas and in the vasculature of the piglet [13,31]. Finally, prostaglandin production in piglet cerebral tissues and vessels is largely reduced by a selective PGHS-2 inhibitor [31]. Similar to piglets, PGHS-2 appears to be particularly prominent in the neonatal rat [43]. The reason for the predominance of PGHS-2 in neurons and glial cells in the perinatal period is unclear, but it has been suggested to be due to augmented synaptic activity during development [1,43,21].

Our findings concerning effects of ischemia on PGHS-2 mRNA and protein levels are consistent with our earlier results as well as those of other laboratories. For example, we have found previously that PGHS-2 but not PGHS-1 levels in cerebral arteries increase [13] and cortical prostaglandin synthetic capacity increases [22] after ischemia in piglets. Our current findings indicate that PGHS-1 mRNA does not increase in brain following ischemic stress in piglets. In addition, Nogawa et al. [29] reported that PGHS-2 mRNA and protein levels increase following permanent, focal ischemia in rats. In their study, levels of mRNA were elevated by 6 h and protein by 12 h. Similarly, Collaço-Moraes et al. [14] reported that PGHS-2 mRNA levels increase by 2 h after permanent, focal ischemia in rats. Major differences between our study and these other studies are that PGHS-2 levels are normally lower in adult rat than piglet brains and they used permanent, focal ischemia while we used transient, global ischemia. Our current findings extend previous studies in 4 ways. First, we examined the effects of anoxic stress on PGHS-2 mRNA and protein in areas other than cortex, such as hippocampus and cerebellum. Second, we documented the cell types in these other regions that are affected by ischemic stress. Third, we examined effects of anoxic stress on the developing brain. And fourth, we showed that ischemia and asphyxia have different effects on the expression of PGHS-2 in brain.

The finding that PGHS-2 mRNA and protein levels in brain increase after ischemia but not after asphyxia was unexpected because both stimuli are equally potent in producing superoxide anion in piglets [32]. In addition, we find that inducible HSP 70 (iHSP 70) increases to a similar extent in brain after both asphyxia and ischemia in brain (unpublished observations). One possible reason for the difference in PGHS-2 responses between ischemia and asphyxia is that in the latter situation systemic levels of CO_2 increase dramatically. Vannucci et al. [39] have reported that exposure to inhaled CO_2 is able to reduce brain damage in neonatal pups following hypoxia–ischemia. In contrast, hypercapnia has been shown to enhance damage during ischemia in adult rats [20,28]. Acidosis can suppress activation of some [17] but not all [44] intermediate early genes. Since PGHS-2 induction in response to hypoxia in endothelial cells is dependent upon activation of NF-kappaβ [34], we speculate that acidosis or some other attribute of asphyxia leads to suppression of this transcription factor.

The attenuation of ischemia-induced increases in PGHS-2 mRNA and protein by indomethacin suggests that products of arachidonic acid metabolism lead to upregulation of PGHS-2. PGHS-dependent production of superoxide anion or of prostanoids during the reperfusion period might activate NF-kappaβ or other transcription factors and lead to enhanced PGHS-2 synthesis [23,34]. For example, indomethacin has also been reported to suppress prostaglandin E_2-induced transcription of corticotropin-releasing hormone [26]. In previous studies, we have shown that indomethacin pretreatment before ischemia attenuates neuronal damage and prevents increases in iHSP70 and endothelial nitric oxide synthase [7,8]. Thus, indomethacin may have a general effect in protecting the brain following ischemic stress and thereby inhibiting increases in stress-induced proteins. Alternatively, indomethacin pretreatment, by preventing production of oxygen radicals during the reperfusion period [32], may prevent reactive oxygen species activation of NF-kappaβ [35]. Since NO can have effects on prostaglandin synthesis or expression of PGHS in vitro [11,18,33], it was surprising that 7-NI had minimal effects on increases in PGHS-2 immunoreactivity after ischemia. However, PGHS-2 immunopositive neurons may not be exposed to sufficiently high levels of brain derived NO since there is little overlap between bNOS and PGHS-2 immunoreactivity in the cerebral cortex and hippocampus in piglets [15]. Alternatively, NO may represent only one of many competing influences on PGHS-2 expression during ischemia/reperfusion.

There are two consequences of increased PGHS-2 levels following ischemia in piglets. First, as we have previously shown [22], prostanoid production of cerebral arteries and tissue are increased following ischemic stress. Thus, prostanoid-mediated effects on the cerebral circulation and/or on brain function might be enhanced after ischemic stress. Second, increased PGHS-2 levels would lead to enhanced superoxide anion production during subsequent neurological sequelae. For example, seizure activity, cessation of breathing, and subarachnoid hemorrhage often occur following resuscitation after hypoxic/ischemic insults in babies [38–40]. Enhanced production of superoxide anion under these conditions [3,6,27,43] might result in further vascular and neuronal damage.

In summary, ischemia increases PGHS-2 but not PGHS-1 levels in cerebral tissues. Elevated levels of PGHS-2 would lead to enhanced capacity for synthesis of prostanoids and superoxide anion in the post-ischemic period, and may result in altered vascular and neuronal function and augmented production of superoxide anion during additional cerebral insults.

Acknowledgements

We thank Drs. K. Peri and S. Chemtob for generously providing the PGHS-1 and PGHS-2 probes for the RNase protection assay and with technical assistance with the assay. In addition, we thank Dr. A.W. Ford-Hutchinson and Dr. S. Prescott for kindly providing the PGHS-2 and PGHS-1 antibodies, respectively.

References

[1] J. Adams, Y. Collaço-Moraes, J. de Belleroche, Cyclooxygenase-2 induction in cerebral cortex: an intracellular response to synaptic excitation, J. Neurochem. 66 (1996) 6–13.

[2] W.M. Armstead, R. Mirro, D.W. Busija, C.W. Leffler, Postischemic generation of superoxide anion by newborn pig brain, Am. J. Physiol. 255 (1988) H401–H403.

[3] W.M. Armstead, R. Mirro, C.W. Leffler, D.W. Busija, Cerebral superoxide anion generation during seizure in newborn pigs, J. Cereb. Blood Flow Metab. 9 (1989) 175–179.

[4] F. Bari, R.A. Errico, T.M. Louis, D.W. Busija, Differential effects of short-term hypoxia and hypercapnia on *N*-methyl-D-aspartate-induced cerebral vasodilatation in piglets, Stroke 27 (1996) 1634–1639.

[5] F. Bari, T.M. Louis, W. Meng, D.W. Busija, Global ischemia impairs ATP-sensitive K^+ channel function in cerebral arterioles in piglets, Stroke 27 (1996) 1874–1881.

[6] F. Bari, R.A. Errico, T.M. Louis, D.W. Busija, Interaction between ATP-sensitive K^+ channels and nitric oxide on pial arterioles in piglets, J. Cereb. Blood Flow Metab. 16 (1996) 1158–1164.

[7] T.C. Beasley, F. Bari, C. Thore, N. Thrikawala, T.M. Louis, D.W. Busija, Cerebral ischemia/reperfusion increases endothelial nitric oxide synthase levels via an indomethacin sensitive mechanisms, J. Cereb. Blood Flow Metab. 18 (1988) 88–96.

[8] T.C. Beasley, F. Bari, C. Thore, N. Thrikawala, T.M. Louis, D.W. Busija. Indomethacin attenuates early induction of cellular injury and iHSP 70 after cerebral ischemia/reperfusion in piglets, Dev. Brain Res., in press.

[9] J.S. Beckman, T.W. Beckman, J. Chen, P.A. Marshall, B.A. Freeman, Apparent hydroxyl radical production by peroxynitrite: implications for endothelial injury from nitric oxide and superoxide, Proc. Natl. Acad. Sci. U.S.A. 87 (1990) 1620–1624.

[10] C.D. Breder, Cyclooxygenase systems in the mammalian brain, Ann. NY Acad. Sci. 813 (1997) 296–301.

[11] D.W. Busija, C. Thore, Modulation of prostaglandin production by nitric oxide in astroglia, Prostaglandins Leukotrienes Fatty Acids 56 (1997) 355–359.

[12] D.W. Busija, W. Meng, Altered cerebrovascular responsiveness to N-methyl-D-aspartate after asphyxia in piglets, Am. J. Physiol. 265 (1993) H389–H394.

[13] D.W. Busija, C. Thore, T. Beasley, F. Bari, Induction of cyclooxygenase-2 following anoxic stress in piglet cerebral arteries, Microcirculation 3 (1996) 379–386.

[14] Y. Collaço-Moraes, B. Aspey, M. Harrison, J. de Belleroche, Cyclo-oxygenase-2 messenger RNA induction in focal cerebral ischemia, J. Cereb. Blood Flow Metab. 16 (1996) 1366–1372.

[15] R. Dégi, F. Bari, T.C. Beasley, N. Thrikawala, C. Thore, D.W. Busija. Regional distribution of prostaglandin H synthase isoforms and neuronal nitric oxide synthase in piglet brain, submitted.

[16] D.L. DeWitt, Prostaglandin endoperoxide synthase: regulation of enzyme expression, Biochem. Biophys. Acta 1083 (1991) 121–134.

[17] K.K. Frick, L. Jiang, D.A. Bushinsky, Acute metabolic acidosis inhibits the induction of osteroblastic egr-1 and type 1 collagen, Am. J. Physiol. 272 (1997) C1450–C1460.

[18] A. Habib, C. Bernard, M. Lebret, C. Creminon, B. Esposito, A. Tedgui, J. Maclouf, Regulation of the expression of cyclooxygenase-2 by nitric oxide in rat peritoneal macrophages, J. Immunol. 158 (1997) 3845–3851.

[19] P.L. Huang, Z. Huang, H. Mashimo, K.D. Bloch, M.A. Moskowitz, M.C. Fishman, Effects of cerebral ischemia in mice deficient in neuronal nitric oxide synthase, Science 265 (1994) 1883–1885.

[20] K. Katsura, T. Kristian, M.L. Smith, B.K. Siesjö, Acidosis induced by hypercapnia exaggerates ischemic brain damage, J. Cereb. Blood Flow Metab. 14 (1994) 243–250.

[21] W.E. Kaufmann, P.F. Worley, J. Pegg, M. Bremer, P. Isakson, Cox-2, a synaptically induced enzyme, is expressed by excitatory neurons at postsynaptic sites in rat cerebral cortex, Proc. Natl. Acad. Sci. U.S.A. 93 (1996) 2317–2321.

[22] C.W. Leffler, R. Mirro, W.M. Armstead, D.W. Busija, Prostanoid synthesis and vascular responses to exogenous arachidonic acid following cerebral ischemia in piglets, Prostaglandins 40 (1990) 241–248.

[23] S.D. Long, P.H. Pekala, Regulation of GLUT4 gene expression by arachidonic acid: evidence for multiple pathways, one of which requires oxidation to prostaglandin E_2, J. Biol. Chem. 271 (1996) 1138–1144.

[24] T.M. Louis, W. Meng, F. Bari, R.A. Errico, D.W. Busija, Ischemia reduces CGRP-induced cerebral vascular dilation in piglets, Stroke 27 (1996) 134–139.

[25] T. Malinski, F. Bailey, Z.G. Zhang, M. Chopp, Nitric oxide measured by a porphyrinic microsensor in rat brain after transient middle cerebral artery occlusion, J. Cereb. Blood Flow Metab. 13 (1993) 355–358.

[26] A.E. Markrigrannakis, E. Zoumakis, A.N. Margioris, C. Stournaras, G.P. Chousos, A. Gravanis, Regulation of the promoter of the human corticotropin-releasing hormone gene in transfected human endometrial cells, Neuroendocrinology 64 (1996) 85–92.

[27] R. Mirro, W.M. Armstead, D.W. Busija, C.W. Leffler, Blood induced superoxide anion generation on the cerebral cortex of newborn pigs, Am. J. Physiol. 257 (1989) H1560–H1564.

[28] Y. Morimoto, T. Yamamura, O. Kemmotsu, Influence of hypoxic and hypercapnic acidosis on brain water content after forebrain ischemia in the rat, Crit. Care Med. 21 (1993) 907–913.

[29] S. Nogawa, F. Zhang, M.E. Ross, C. Iadecola, Cyclo-oxygenase-2 gene expression in neurons contributes to ischemic brain damage, J. Neurosci. 17 (1997) 2746–2755.

[30] H. Parfenova, T.H. Eidson, C.W. Leffler, Upregulation of COX-2 in cerebral microvascular endothelial cells by smooth muscle cell signals, Am. J. Physiol. 273 (1997) C277–C288.

[31] K.G. Peri, P. Hardy, D.Y. Li, D.R. Varma, S. Chemtob, Prostaglandin G/H synthase-2 is a major contributor of brain prostaglandins in the newborn, J. Biol. Chem. 270 (1995) 24615–24620.

[32] M. Pourcyrous, C.W. Leffler, H.S. Bada, S.B. Korones, D.W. Busija, Brain superoxide anion generation in asphyxiated piglets and the effect of indomethacin at therapeutic dose, Pediatr. Res. 34 (1993) 366–369.

[33] D. Salvemini, T.P. Misko, J.L. Masferrer, K. Seibert, M.G. Currie, P. Needleman, Nitric oxide activates cyclooxygenase enzymes, Proc. Natl. Acad. Sci. U.S.A. 90 (1993) 7240–7244.

[34] J.F. Schmedtje Jr., Y.S. Ji, W.L. Liu, R.N. DuBois, M.S. Runge, Hypoxia induces cyclooxygenase-2 via the NF-kappaB p65 transcription factor in human vascular endothelial cells, J. Biol. Chem. 272 (1997) 601–608.

[35] C.K. Sen, L. Packer, Antioxidant and redox regulation of gene transcription, FASEB J. 10 (1996) 709–720.

[36] W.L. Smith, Prostanoid biosynthesis and mechanisms of action, Am. J. Physiol. 263 (1992) F181–F191.

[37] W.K.M. Tan, C.E. Williams, M.J. During, C.E. Mallard, M.I. Gunning, A.J. Gunn, P.D. Gluckman, Accumulation of cytotoxins during the development of seizures and edema after hypoxic-ischemic injury in last gestational fetal sheep, Pediatr. Res. 39 (1996) 791–797.

[38] R.C. Vannucci, Perinatal hypoxic/ischemic encephalopathy, Neurologist 1 (1995) 35–52.
[39] R.C. Vannucci, J. Towfighi, D.F. Heitjan, R.M. Brucklacher, Carbon dioxide protects the perinatal brain from hypoxic-ischemic damage: an experimental study in the immature rat, Pediatrics 95 (1995) 868–874.
[40] J.J. Volpe, Brain injury in the premature infant—current concepts, Prev. Med. 23 (1994) 638–645.
[41] C.E. Williams, A.J. Gunn, C. Mallard, P.D. Gluckman, Outcome after ischemia in the developing sheep brain: an electroencephalographic and histological study, Ann. Neurol. 31 (1992) 14–21.
[42] K.K. Wu, Cyclooxygenase 2 induction: molecular mechanism and pathophysiologic roles, J. Lab. Clin. Med. 128 (1996) 242–245.
[43] K. Yamagata, K.I. Andreasson, W.E. Kaufmann, C.A. Barnes, P.F. Worley, Expression of a mitogen-inducible cyclooxygenase in brain neurons: regulation by synaptic activity and glucocorticoids, Neuron 11 (1993) 371–386.
[44] Y. Yamaji, O.W. Moe, R.T. Miller, R.J. Alpern, Acid activation of immediate early genes in renal epithelial cells, J. Clin. Invest. 94 (1994) 1297–1303.
[45] Z.G. Zhang, D. Reif, J. Macdonald, W.X. Tang, D.K. Kamp, R.J. Gentile, W.C. Shakespeare, R.J. Murray, M. Chopp, ARL 17477, a potent and selective neuronal NOS inhibitor, decreases infarct volume after transient middle cerebral artery occlusion in rats, J. Cereb. Blood Flow Metab. 16 (1996) 599–604.

III

Graefe's Arch Clin Exp Ophthalmol (2001)
239:59–65

LABORATORY INVESTIGATION

Rózsa Dégi
Clara Thore
Ferenc Bari
Nishadi Thrikawala
Antal Nógrádi
Greg Robins
Ferenc Domoki
Tracy C. Beasley
David W. Busija

Ischemia increases prostaglandin H synthase-2 levels in retina and visual cortex in piglets

Received: 21 March 2000
Revised: 12 September 2000
Accepted: 20 September 2000

R. Dégi · C. Thore · F. Bari · N. Thrikawala
G. Robins. F. Domoki · T.C. Beasley
D.W. Busija (✉)
Department of Physiology
and Pharmacology,
Wake Forest University
School of Medicine,
Medical Center Boulevard,
Winston-Salem, NC 27157-1083, USA
e-mail: dbusija@wfubmc.edu
Tel.: +1-336-7164355
Fax: +1-336-7160237

R. Dégi · A. Nógrádi
Department of Ophthalmology,
Albert Szent-Györgyi Medical University,
Szeged, Hungary

F. Bari · F. Domoki
Department of Physiology,
Albert Szent-Györgyi Medical University,
Szeged, Hungary

Abstract *Background:* Ischemia increases levels of prostaglandin H synthase-2 (PGHS-2) in neonatal brain and cerebral vasculature, but effects on the developing visual system are unknown. We examined the effects of ischemia on PGHS-2 mRNA and protein levels in the retina and visual cortex in anesthetized piglets. *Methods:* Ten minutes of complete retinal and brain ischemia was induced by increasing intracranial pressure. After 2–12 h of reperfusion, samples of retina and visual cortex were collected for determinations of levels of PGHS-2 mRNA (RNase protection assay) or protein (immunohistochemistry and western blotting). Tissues also were obtained from control animals.
Results: Levels of PGHS-2 mRNA were undetectable in control animals but showed a dramatic increase at 2–4 h in the cortex and retina in animals exposed to ischemia. Detectable but limited PGHS-2 immunoreactivity (IR) was present in the retina and visual cortex from control animals. In piglets not subjected to ischemia, PGHS-2 IR was localized mainly to the outer limiting membrane and to the Müller cells. Ischemia induced a marked increase in PGHS-2 IR in the neural retina, with the greatest increase in the photoreceptor layer. PGHS-2 levels in whole retina also increased at 8 h after ischemia. In the intact visual cortex PGHS-2 IR was evident in layers II and V. Ischemia increased the intensity of IR in layers II/III as well as layer V. *Conclusions:* Detectable amounts of PGHS-2 protein are present in the piglet retina and visual cortex under normal conditions, but levels are markedly increased 8–12 h after ischemic stress. Enhanced PGHS-2 levels after ischemic stress may contribute to delayed pathological changes of the visual system in the neonate.

Introduction

Metabolites of prostaglandin H synthase (PGHS; commonly referred to as cyclooxygenase), including prostanoids (prostaglandins and thromboxane) and superoxide anion, are involved in the physiology and pathophysiology of the visual system [5, 6, 11, 19]. The retina and visual cortex contain considerable amounts of membrane-bound arachidonic acid, which can be released under a variety of conditions. In addition, the retina exhibits PGHS activity and synthesizes all major prostaglandins [16]. Prostaglandin synthesis in the retina can be activated by several conditions, such as exposure to high-intensity visible light [8]. Further, prostaglandin E_2 (PGE_2) and $PGF_{2\alpha}$ receptors are located on the retinal blood vessels, whereas PGE_2 and PGD_2 binding sites are present on various cell types, including photoreceptors, bipolar, horizontal, ganglion and Müller cells [20, 22, 24]. Arachidonic acid metabolites, possibly including prostanoids, also participate in the control of the retinal blood flow [1, 2, 10]. Similarly, PGHS-derived metabolites would be expected to participate in neuronal and

vascular responses in the visual cortex [27]. Finally, production of large amounts of superoxide anion via the PGHS pathway after conditions such as hypoxic–ischemic stress are able to damage neurons and to modify responsiveness of retinal and cerebral blood vessels [4, 17].

Two isoforms of PGHS have been isolated which are very similar in structure and catalytic activity. The PGHS-1 isoform has been regarded as the constitutive variety and thus is present during normal conditions. The PGHS-2 isoform is normally not present in most tissues, but PGHS-2 levels can increase rapidly in response to a number of stresses. However, recent findings from our laboratory and from other laboratories indicate that PGHS-2 is the predominant isoform under normal conditions and that levels increase dramatically following ischemic stress in the brain and cerebral vasculature of the newborn pig [9, 13–15, 25]. Similar findings concerning PGHS-2 have been reported for the adult brain of several species, thereby indicating that neural tissues may be unique with respect to the expression of this isoform. The extent and distribution of PGHS-2 in the retina are unknown.

Stress-induced alterations in the levels of PGHS may have dramatic effects on the developing retina and visual cortex in the neonate. For example, augmented PGHS levels leading to an increase in production of prostanoids and superoxide anion may result in disrupted cellular relationships, abnormal functioning of neural tissues, inappropriate blood flow responses and/or enhanced cell damage and apoptosis following pathological conditions [1, 3, 19]. However, changes in PGHS levels in the visual system have not been previously examined in the neonate.

The purpose of this study was to examine regulation of PGHS-2 in the retina and visual cortex of the newborn pig. We tested the hypotheses that PGHS-2 is constitutively expressed in the retina and in the visual cortex, and that transient cerebral ischemia causes rapid increases of PGHS-2 levels in these tissues. We chose to study this animal model because hypoxic–ischemic stress occurs relatively commonly in human babies and because of the potential damage of this type of stress on the developing visual system.

Material and methods

Animals and surgical procedures

All procedures were approved by the Animal Care and Use Committee at the Wake Forest University School of Medicine, and conform to the "Principles of Laboratory Animal Care" as defined in National Institutes of Health (USA) publications. Newborn (1- to 6-day-old) pigs of either sex weighing between 0.8 and 1.4 kg were used. Surgical procedures have been described in detail previously [13]. Briefly, anesthesia was induced with sodium thiopental (35–40 mg/kg, i.p.) and maintained with α-chloralose (75 mg/kg initial dose and 15–20 mg/kg/h, i.v.). Blood pressure and body temperature were monitored throughout the experiment. Animals were artificially ventilated with room air. Ventilation parameters were set to maintain arterial pH, pCO_2 and pO_2 within normal values (7.35–7.45, 30–35 mmHg and 80–100 mmHg, respectively) throughout the experiments. Anesthetized, instrumented piglets were divided into ischemia and time-control groups. Total cerebral ischemia was induced and maintained by the infusion of artificial cerebrospinal fluid into the cranium, resulting in an increase in intracranial pressure. Venous blood was withdrawn as necessary during this procedure to maintain normal mean arterial pressure. Cessation of cerebral blood flow was verified visually via a microscope positioned over a closed glass and stainless steel cranial window implanted above the surface of the cerebral cortex. After 10 min of ischemia, the infusion tube was clamped, intracranial pressure allowed to normalize, and venous blood returned. Time-control animals were treated like the other group, but were not exposed to ischemia. Animals were killed under anesthesia with intravenous KCl at 1, 2, 4, 6, 8 and 12 h after ischemia and the eyes and visual cortex were removed for immunohistochemistry or biochemical measurements (n=18 for ischemia and n=18 for time-control animals). Tissue samples were also obtained from untreated, killed control animals (n=4).

Previous experiments indicate that blood flow to the entire brain and other areas of the central nervous system such as the spinal cord becomes undetectable during increased intracranial pressure [7, 23]. To evaluate effects of increased intracranial pressure on blood flow to the retina, we injected 15-μm microspheres in two animals during control conditions and during increased intracranial pressure. Equal numbers of green or orange microspheres were injected into the left ventricle, where they mixed with the blood and were distributed to tissues in proportion to blood flow. The microspheres stay trapped in the microcirculation even after additional interventions. After intracranial pressure was returned to normal, the animals were killed and both retinas and samples of visual cortex from both sides of the brain were removed. The tissues were chemically digested and the microspheres extracted and counted. Under control conditions, there were 176±37 microspheres per gram in retina (n=4) and 216±27 microspheres per gram in cortex (n=4). Under conditions of increased intracranial pressure, no microspheres were detected in either retina or cortex. Thus, blood flow to the retina and cortex was reduced to non-detectable levels at this time.

Immunohistochemistry

Eyes were opened at the corneal-scleral border with a sharp blade and placed in neutral buffered formalin. After fixation, the neural retina was removed with fine forceps, washed thoroughly in 10 mM phosphate buffer/0.9% saline, pH 7.4 (PBS), embedded in OCT and stored at –60° C until cryostat sectioning. Occipital cortex was immersion-fixed overnight in the same fixative, washed in PBS and stored at 4° C until sectioned on a vibratome.

Sections of visual cortex (50 μm) and retina (8 μm) were stained free-floating using a three-step immunoperoxidase method. All washes were done in PBS between each step unless stated otherwise. Detailed procedures for the immunohistochemistry have been previously published [13–15, 26]. Briefly, sections were pretreated with ammonium chloride for 1 h and incubated in 0.3% Triton-X 100 for 1 h. Endogenous peroxidases were blocked by incubation of the sections in 3% H_2O_2/MetOH. The sections were then blocked in 10% normal goat serum (NGS)/0.1% Tween-20 for 2 h followed by an overnight incubation in PGHS-2 primary antibody (Dr. A.W. Ford-Hutchinson, Merck Frosst Center for Therapeutic Research, Pointe Claire, Quebec, Canada) at a dilution of 1:2,000. The antiserum was diluted in 2% NGS/0.1% Tween. Subsequently, the sections were incubated in biotinylated goat anti-rabbit antibody (Vector, Burlingame, Calif.) at a dilution

of 1:1,000 for 2 h. Finally, the sections were reacted with ABC reagent (Vector) for 30 min and with diaminobenzidine (DAB; Vector). Retina was mounted on glass slides and coverslipped in glycerol. Occipital cortex was mounted, dehydrated and coverslipped with a toluene-based mounting medium. General morphology of the retina was examined on cresyl violet and/or hematoxylin-eosin stained sections. Analysis and photomicroscopy were done with a Zeiss Axioskop microscope (Jena, Germany). Publication figures were created digitally from original slides and negatives, with care to reproduce the appearance of the original images.

Immunoblot analysis

Protein was extracted from frozen retinas in boiling lysis buffer (10 mmol/l Tris and 1% SDS). The samples were sonicated, heated at 95° C for 5 min, and centrifuged for 15 min at 12,000 rpm at 4° C. An aliquot of the supernatant was removed for protein concentration determination. After the addition of an equal volume of sample buffer (100 mmol/l Tris, pH 6.8; 42% glycerol; 5% bromophenol blue; and 1% SDS) to each sample, the protein was separated on a 4–20% gradient mini gel (Bio-Rad, N.Y.) and transferred to nitrocellulose. After non-specific protein binding was blocked by incubating the blot in 5% milk, primary antibody against PGHS-2 (1:1,000) was applied, followed by horseradish peroxidase-conjugated secondary antibody (1:10,000) (goat anti-rabbit, Jackson Immunoresearch, Pa.). Electrochemiluminescence was used to visualize the bands. Molecular weight markers were also run.

RNase protection assay

Samples of occipital cortex and retina were frozen immediately in 2-methyl butane at 70° C prior to storage at –60° C until processing. Total RNA was extracted from frozen samples by guanidium/phenol-chloroform-isoamyl alcohol extraction and ethanol precipitation. Twenty-five micrograms of total RNA from each retinal or cortical tissue sample was assayed using an RNase protection assay kit (RPA II; Ambion, Austin, Tex.). Sense and antisense ^{32}P-labeled riboprobes were transcribed from porcine specific PGHS-2 cDNA [25] with the MaxiScript kit (Ambion). After hybridization and RNase digestion, protected fragments were resolved on a 6% urea/acrylamide gel and autoradiographed using Hyperfilm (Amersham, Arlington Heights, Ill.).

Results

A section of retina stained with cresyl violet is shown in Fig. 1A for orientation. From the outside inward, seven layers are discernable. These are the photoreceptor layer (P), the outer nuclear layer (ONL), the outer plexiform layer (OPL), the inner nuclear layer (INL), the inner plexiform layer (IPL), the layer of ganglion cells (G) and the layer of optic nerve fibers (NFL). A clearly discernible outer limiting membrane (OLM) is also located between P and ONL (Fig. 1D, arrowheads).

Limited but detectable immunostaining for PGHS-2 was present in control retinas and was layer-dependent. There were no major differences in immunostaining patterns between untreated and time-control retinas (data not shown). Intact retinas immunostained for PGHS-2 are shown in Fig. 1B-E (negative control is shown in in-

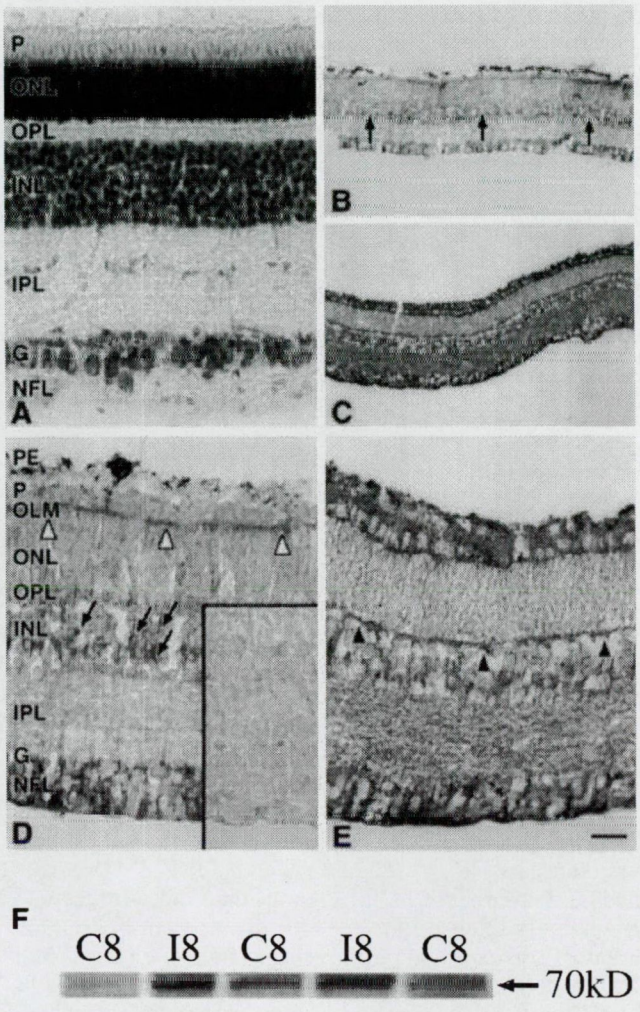

Fig. 1A–F Effects of ischemia on PGHS-2 immunoreactivity (IR) and immunoblotting of the piglet retina. **A** The laminar organization of the piglet retina after cresyl violet staining. Labels indicate photoreceptor (*P*), outer nuclear (*ONL*), outer plexiform (*OPL*); inner nuclear (*INL*), inner plexiform (*IPL*), ganglion cell (*G*), and nerve fiber (*NFL*) layers. **B–E** Retinal sections stained for PGHS-2. **B, D** Low and high magnifications, respectively, of retina from untreated piglet. *Arrows* represent relatively heavy PGHS-2 immunostaining in cell bodies within the INL, which probably are Müller cells. *White arrowheads* indicate presence of PGHS-2 immunostaining in OLM. Moderate PGHS-2 IR is also associated with layers G and NFL. *Insert* demonstrates lack of immunostaining in a preimmune, control retina. *PE* Pigment epithelium, *OLM* outer limiting membrane. **C, E** Low and high magnifications, respectively, of retina from a piglet 12 h after ischemia. Obvious increases in PGHS-2 IR occur in P, OLM, OPL/INL interface (*dark arrowheads*), G, and NFL. The lack of increased immunostaining in the ONL after ischemia caused this layer to appear relatively unstained compared with the other retinal layers (compare **B** and **C**). *Scale bar:* **A, D, E** 100 μm; **B, C** 400 μm; insert in **D** 66.6 μm. **F** There were increases in PGHS-2 protein levels 8 h after ischemia in whole retina via immunoblotting. The immunoreactive band migrated at the appropriate molecular weight for PGHS-2, and previous studies have shown that pre-adsorption eliminated the band at this location

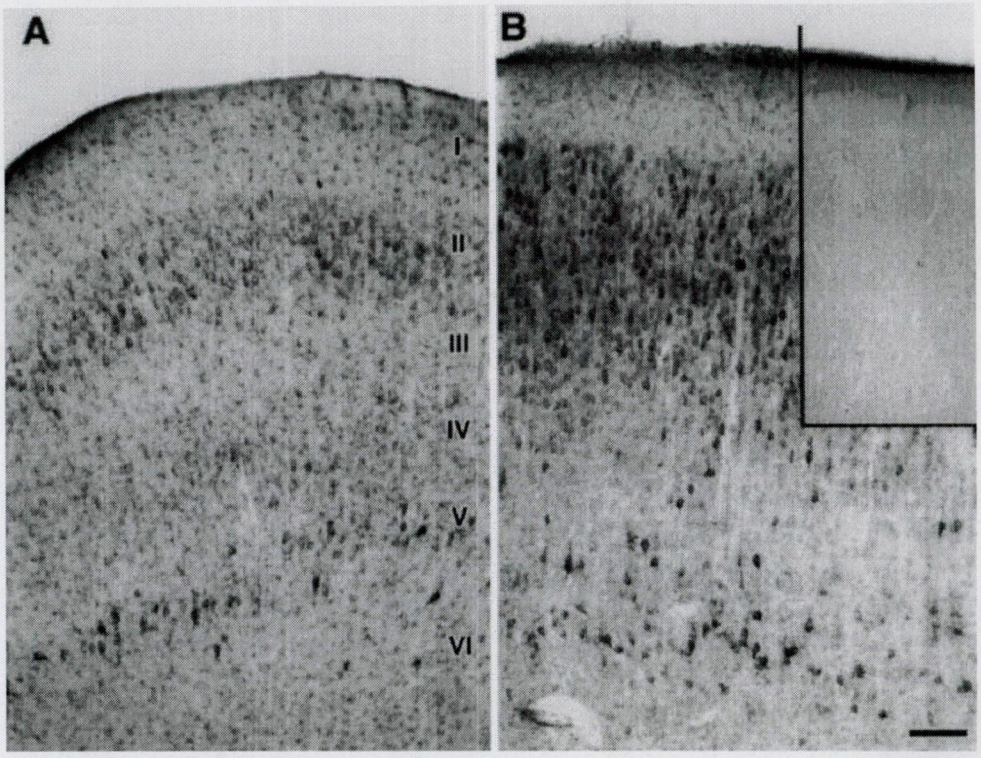

Fig. 2A, B Effects of ischemic stress on visual cortex PGHS-2 IR. **A** Modest PGHS-2 IR in scattered neurons localized to cortical layers II and V in a section from an 8-h time control animal. *Roman numerals* indicate cortical layers. **B** Increased PGHS-2 IR was observed in a section 8 h after cerebral ischemia. The most prominent changes in IR were in layers II/III, but an increase in labeled neurons also was prominent in layers V. *Insert*: Only minimal background PGHS-2 IR was seen in section of visual cortex following preadsorption of PGHS-2 antisera with purified PGHS-2 antigen. *Scale bar:* 100 μm

sert in Fig. 1D). Untreated retina exhibited PGHS-2 immunoreactivity (IR) localized to the OLM (Fig. 1D, arrowheads), with diffuse IR throughout the ONL/OPL region. Moderately intense staining was also evident in scattered areas of the ganglion cell layer and in a line of cell bodies located in the INL midline. The location and morphology of these immunoreactive cells suggested that they corresponded to Müller cells. The INL staining appears as a discontinuous chain (arrowheads) of IR coursing through the INL (arrows) in the lower magnification (Fig. 1B, D). No PGHS-2 IR was seen in other retinal layers above the background level. Preimmune technical control sections of retina revealed no detectable PGHS-2 IR (Fig. 1D, insert). Very dark areas at the surface of the photoreceptor layer (most noticeable in Fig. 1B, D) are fragments of pigment epithelium (PE) which were still present in some sections.

Ischemia induced a marked increase in PGHS-2 IR in the neural retina (Fig. 1C, E). After 8 h (data not shown) or 12 h recovery from 10 min of ischemia, immunoreactive PGHS-2 was elevated in all layers of the retina except ONL/OPL, with the greatest increases seen throughout the photoreceptor layer including the OLM. PGHS IR was distributed in some areas along the full length of the photoreceptors into the outer segments. Also, a discontinuous row of immunoreactive PGHS-2 elements became apparent after ischemia in the vicinity of the OPL/INL interface that was not seen in untreated or time-control retinas. It is particularly evident in the low magnification view in Fig. 1C. The absence of significant PGHS-2 IR in the ONL after ischemia caused this layer to appear unstained compared with the increased IR of other retinal layers.

Müller cell PGHS-2 IR (arrows in Fig. 1B, D) also appeared to be increasing, as evidenced by an increase in cytoplasmic IR in cell soma located midline in INL and in basal and apical membranes, but these increases were more subtle. Moderate to substantial PGHS IR was present in the IPL, G and NFL layers.

Immunoblotting using whole retina supported the immunostaining results (Fig. 1F). Thus, PGHS-2 protein in whole retina increased dramatically by 8 h after ischemia.

Sections of visual cortex from a time-control animal and from an animal 8 h after the induction of global cerebral ischemia are shown in Fig. 2. Preadsorption of the antisera with purified PGHS-2 before incubation with sections resulted in low background IR and no identifiable neuronal structures (Fig. 2A). Time-control cortex contained immunoreactive PGHS-2 neurons located primarily in cortical layers II and V. However, some PGHS-2 IR neurons were scattered throughout the gray matter of visual cortex in definite layers. Neuronal PGHS IR increased markedly, especially in cortical layers II/III and V, 8 h after ischemia (Fig. 2B). Increases in both the staining intensity of individual neurons and the

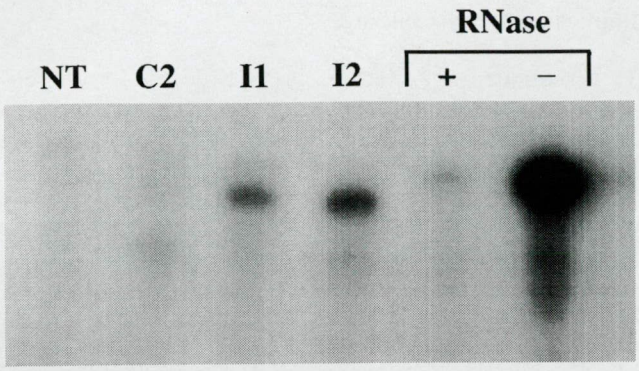

Fig. 3 PGHS-2 mRNA expression in the piglet retina after ischemia. Autoradiograph from RNase protection assay illustrates very low PGHS mRNA levels from a naive control (*NT*) and from a 2-h time-control animal (*C2*). Expression of PGHS-2 mRNA is increased 1 h and 2 h after ischemia (*I1* and *I2*). Unhybridized anti-sense probe digested with RNase is shown in the "+" lane, while unhybridized, undigested anti-sense probe is shown in the "–" lane. The unhybridized probe band shown in the last lane runs at 209 bp and the hybridized, protected fragments migrate at 185 bp

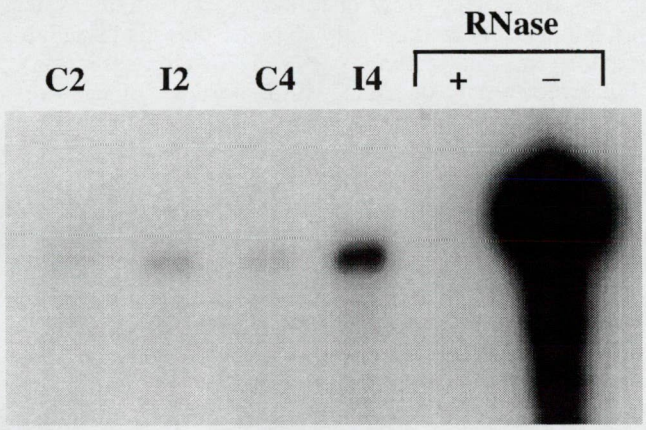

Fig. 4 Upregulation of PGHS-2 mRNA in the visual cortex after ischemia. RNase protection assay revealed increased expression of PGHS-2 mRNA in the occipital cortex in animals surviving 2 and 4 h after ischemia (*I2* and *I4*). The 2-h and 4-h time-controls are indicated as *C2* and *C4*. Unhybridized probe digested with RNase is shown in the "+" lane, while the unhybridized, undigested probe is shown in the "–" lane.

number of PGHS-2 IR neurons were apparent. Subcellularly, PGHS IR filled the cytoplasm and was concentrated in perinuclear areas of the neuronal soma, extending into the apical dendrite in very heavily stained neurons (not shown).

PGHS-2 mRNA was barely detectable in the non-treated or time-control retina at 2 h, but by 1 h and 2 h after ischemia levels had increased considerably (Fig. 3). At 4 h after ischemia, mRNA levels were not different from 1-hr control values (data not shown).

PGHS-2 mRNA levels were barely detectable in the non-treated or time-control retina at 2 h in the occipital cortex (Fig. 4), but levels increased after ischemia and reached maximum values by 4 h. In technical control experiments, no bands were evident in those lanes where total RNA samples were hybridized with sense riboprobes transcribed from the cDNA template (data not shown).

Discussion

There are two major findings of this study. First, detectable amounts of PGHS-2 are present in the retina and the visual cortex of intact newborn pig. Second, transient ischemic stress leads to enhanced levels of PGHS-2 mRNA within 2–4 h and PGHS-2 protein within 8–12 h. Our current results confirm and extend previous findings by our laboratory indicating that PGHS-2 protein synthesis is very sensitive to ischemic stress in the piglet central nervous system. Further, increased levels of PGHS-2 in retina and occipital cortex will probably affect function, maturation and susceptibility to stress in the visual system of the developing animal.

Consideration of methods

Immunohistochemical characteristics of PGHS-2 observed in the present experiments are consistent with results from our previous in vitro [26] and in vivo [14] studies. For example, PGHS-2 is present constitutively to varying extents in the neurons and glial cells of the developing central nervous system. In addition, PGHS-2 is concentrated in perinuclear areas as well as dendrites of neurons and terminal processes of astroglia. Further, changes in PGHS-2 IR are specific and do not involve all cell types, and responses in similar cell populations are variable. Finally, increases in PGHS-2 mRNA and protein are relatively rapid and occur within a few hours.

We have assessed the specificity of the PGHS-2 antibody and other reagents used in immunostaining using several procedures. First, we have shown similar immunostaining between this and another PGHS-2 antibody from a different source, and use of either of these antibodies showed a different staining pattern than that obtained using PGHS-1 antibodies [13–15, 26]. Second, PGHS-2 immunostaining was eliminated following preadsorption with purified PGHS-2. Third, use of preimmune serum or elimination of the PGHS-2 antibody shows minimal staining. Fourth, western blotting results in cerebral blood vessels [15] supported results from PGHS-2 immunostaining experiments. In the current study, we have shown that western blotting and immunohistochemistry support the conclusion that ischemic stress increases PGHS-2 protein levels in the retina.

Consideration of results

The PGHS-2 IR pattern of the control retina was such that most immunopositive staining appeared in four regions, three of which are known to be associated with the Müller cell: (1) in a diffuse line at the level of the OLM, (2) in cell soma located midline in the INL, (3) in pockets of IR between ganglion cell nuclei, and (4) scattered IR throughout the ONL/OPL. The OLM marks the apical pole of the Müller cell, a bipolar cell that spans the entire thickness of the retina from the basal membrane to the photoreceptor layer. The nuclei of Müller cells are located within the INL, where they form a distinct median sublayer. Thus, PGHS-2 IR was seen in areas corresponding to the Müller cell soma and at the termination of both outer and inner processes. The diffuse IR seen in the OPL/ONL region could be localized to only two cell types, photoreceptor cell bodies, which are located in the ONL, and the Müller cell, which at this level forms velate sheaths around photoreceptor cell nuclei. Although double immunostaining for GFAP/PGHS-2 was not carried out, it is likely that these immunoreactive cells are Müller cell somata based on location and morphological features. The IR seen at the OLM border and in the ganglionic layer is probably due to PGHS-2 in Müller cell processes. Little PGHS-2 IR was apparent in the other neuronal cell types of the retina – the horizontal cell, the amacrine cell and the retinal ganglion cell – at least in the perinuclear areas.

Ischemia had dramatic but variable effects on retinal staining. For example, neurons and Müller cells showed enhanced PGHS-2 IR, while perinuclear areas of the photoreceptor cells showed little IR. In contrast, changes in PGHS-2 distribution in retinal neuronal elements after ischemia were more dramatic. After ischemia a discontinuous line of PGHS-2 IR was apparent in the OPL/INL interface. Known to occupy this region are the dendritic fields of bipolar neurons and horizontal cells, and the linear pattern of IR might be due to increased PGHS-2 in the dendritic fields of either or both cell types. The modest increase in IR seen in the other synaptic region of the retina, the IPL, could also be attributed to the dendritic field of other retinal neurons, the amacrine cells, whose soma are located in the ONL or cell bodies of ganglion cells. Alternatively, Müller cells are known to extend horizontal branches into this synaptic region, and indeed the IR appears to have a horizontal pattern in the low-magnification aspect seen in Fig. 1C.

As we have reported previously in parietal cortex [13], PGHS-2 IR is widespread in the visual cortex during control conditions. Following ischemia, PGHS-2 IR increased dramatically in layers II-V, especially in pyramidal neurons. Staining was primarily perinuclear and also evident in the proximal portion of the apical process of heavily PGHS-2 immunoreactive neurons.

Implications of the findings

The consequences of increased PGHS levels for the retina and visual cortex following ischemic stress are unknown. However, based upon our previous work and that of others, several important effects may be expected. Augmented levels of PGHS with resultant increases in production of prostanoids and superoxide anion may lead to disrupted cellular relationships, abnormal functioning of neural tissues, inappropriate blood flow responses, and/or enhanced cell damage following additional pathological conditions [2, 3, 17, 19]. For example, elevated levels of retinal PGHS would be expected to increase superoxide anion production when exposed to short-wavelength visible light, resulting in altered retinal electrophysiology and photic-induced retinal injury [18]. Similarly, PGHS-derived PGE_2 would stimulate expression of angiogenic factors in Müller cells and may result in retinal neovascularization after hypoxic–ischemic injury [12]. In addition, altered PGHS levels could disrupt the balance between dilator nitric oxide and constrictor prostaglandins and thromboxane in maintaining appropriate blood flow in retina [1, 28]. Finally, since PGHS-2 levels are normally spatially correlated with excitatory synaptic activity, generalized overexpression of this isoform may interfere with maturation of individual neurons and with the establishment of interneuronal connections in the developing brain [21].

Hypoxic–ischemic injury is a relatively common occurrence in the perinatal period, and is associated with immediate and sustained damage to the visual system. Our findings provide a basis for suggesting that augmented PGHS-2 levels occurring following ischemic stress may participate in the progression of these neuronal and retinal pathological processes. Nonetheless, more work is needed to establish a causative relationship between increased PGHS-2 levels and cellular vulnerability in the developing visual system.

In summary, PGHS-2 is normally present in the retina and the visual cortex of the newborn pig, although the distribution of this enzyme is limited. However, global cerebral ischemia results in increased levels of PGHS-2 mRNA and protein within 2–8 h. The enhanced levels of PGHS-2 could represent a major source of free radicals and of prostaglandins and thromboxanes in the injured brain, and may lead to disruption of cellular and vascular function and promote injury in the retina and visual cortex.

Acknowledgments This study was supported by grants HL-30260, HL-30260 and HL-50587 from the National Institute of Health, and by grants from the OTKA-T-02 6295 and ETT-T-07614/97 (Hungary). We thank Drs. K. Peri and S. Chemtob for generously providing the PGHS-2 probe for the RNase protection assay and for technical advice. In addition, we thank Dr. A.W. Ford-Hutchinson for kindly providing the PGHS-2 antibody. Finally, we thank Mr. Dwight Deal for help with the microsphere experiments.

References

1. Abran D, Varma DR, Li DY, Chemtob S (1994) Reduced responses of retinal vessels of the newborn pig to prostaglandins but not to thromboxane. Can J Physiol Pharmacol 72: 168–173
2. Abran D, Varma DR, Chemtob S (1995) Increased thromboxane-mediated contractions of retinal vessels of newborn pigs to peroxides. Am J Physiol 268: H628–632
3. al-Zadjali KH, Imler MP, Ohia SE (1994) Inhibitory effect of prostaglandins on dopamine release from the retina. Gen Pharmacol 25: 289–296
4. Bari F, Louis TM, Meng W, Busija DW (1996) Global ischemia impairs ATP-sensitive K^+ channel function in cerebral arterioles in piglets. Stroke 27: 1874–1880
5. Bazan NG (1989) Metabolism of arachidonic acid in the retina and retinal pigment epithelium: biological effects of oxygenated metabolites of arachidonic acid. In: Bito LZ, Stiernschantz J (eds) The ocular effects of prostaglandins and other eicosanoids. Liss, New York, pp 15–37
6. Bazan NG, Allan G (1997) Signal transduction and gene expression in the eye: a contemporary view of the pro-inflammatory, anti-inflammatory and modulatory roles of prostaglandins and other bioactive lipids. Surv Ophthalmol 41 [Suppl 2]: S23–34
7. Beasley TC, Bari F, Thore C, Thrikawala N, Louis T, Busija D (1998) Cerebral ischemia/reperfusion increases endothelial nitric oxide synthase levels by an indomethacin-sensitive mechanism. J Cereb Blood Flow Metab 18: 88–96
8. Birkle DL, Bazan NG (1989) Light exposure stimulates arachidonic acid metabolism in intact rat retina and isolated rod outer segments. Neurochem Res 14: 5–90
9. Busija DW, Thore C, Beasley T, Bari F (1996) Induction of cyclooxygenase-2 following anoxic stress in piglet cerebral arteries. Microcirculation 3: 379–386
10. Chemtob S, Beharry K, Rex J, Chatterjee T, Varma DR, Aranda JV (1991) Ibuprofen enhances retinal and choroidal blood flow autoregulation in newborn piglets. Invest Ophthalmol 32: 1799–1807
11. Chemtob S, Roy MS, Abran D, Fernandez H, Varma DR (1993) Prevention of postasphyxial increase in lipid peroxides and retinal function deterioration in the newborn pig by inhibition of cyclooxygenase activity and free radical generation. Pediatric Res 33: 336–340
12. Cheng T, Cao W, Wen R, Steinberg RH, LaVail MM (1998) Prostaglandin E_2 induces vascular endothelial growth factor and basic fibroblast growth factor mRNA expression in cultured rat Müller cells. Invest Ophthalmol 39: 581–591
13. Dégi R, Bari F, Beasley TC, Thrikawala N, Thore C, Louis TM, Busija DW (1998a) Regional distribution of prostaglandin H synthase-2 and neuronal nitric oxide synthase in piglet brain. Pediatric Res 43: 683–689
14. Dégi R, Bari F, Thrikawala N, Beasley TC, Thore C, Louis TM, Busija DW (1998b) Effects of anoxic stress on prostaglandin H synthase isoforms in piglet brain. Dev Brain Res 107: 265–276
15. Domoki F, Veltkamp R, Thrikawala N, Robins G, Bari F, Louis TM, Busija DW (1999) Ischemia-reperfusion rapidly increases COX-2 expression in piglet cerebral arteries. Am J Physiol 277: H1207-H1214
16. Goh Y, Urade Y, Fujimoto N, Hayaishi O (1987) Content and formation of prostaglandins and distribution of prostaglandin-related enzyme activities in the rat ocular system. Biochim Biophys Acta 921:302–311
17. Hall ED, Yonkers PA, Andrus PK, Cox JW, Anderson DK (1992) Biochemistry and pharmacology of lipid antioxidants in acute brain and spinal cord injury. J Neurotrauma 9 [Suppl 2]: S425–442
18. Hanna N, Peri KG, Abran D, Hardy P, Doke A, Lachapelle P, Roy MS, Orquin J, Varma DR, Chemtob S (1997) Light induces peroxidation in retina by activating prostaglandin G/H synthase. Free Radic Biol Med 23: 885–897
19. Hardy P, Abran D, Li DY, Fernandez H, Varma DR, Chemtob S (1994) Free radicals in retinal and choroidal blood flow autoregulation in the piglet: interaction with prostaglandins. Invest Ophthalmol 35: 580–591
20. Hardy P, Bhatthacharya M, Abran D, Peri KG, Asselin P, Varma DR, Chemtob S (1998) Increases in retinovascular prostaglandin receptor functions by cyclooxygenase-1 and -2 inhibition. Invest Ophthalmol 39: 1888–1898
21. Kaufmann WE, Worley PF, Taylor CV, Bremer M, Jackson PC (1997) Cyclooxygenase-2 expression during rat neocortical development and in Rett syndrome. Brain Dev 19: 25–34
22. Kulkami P, Payne S (1997) Eicosanoids in bovine retinal microcirculation. J Ocul Pharmacol Ther 13: 139–149
23. Leffler CW, Busija DW, Mirro R, Armstead WM, Beasley DG (1989) Effects of ischemia on brain blood flow and oxygen consumption of newborn pigs. Am J Physiol 257: H1917-H1926
24. Matsuo T, Cynader MS (1992) Localization of prostaglandin F_2 alpha and E_2 binding sites in the human eye. Br J Ophthalmol 76: 210–213
25. Peri KG, Hardy P, Li DY, Varma DR, Chemtob S (1995) Prostaglandin G/H synthase-2 is a major contributor of brain prostaglandins in the newborn. J Biol Chem 270: 24615–24620
26. Thore CR, Beasley TC, Busija DW (1998) In vitro and in vivo localization of prostaglandin H synthase in fetal sheep neurons. Neurosci Lett 242: 29–32
27. Yamagata K, Andreasson KI, Kaufmann WE, Barnes CA, Worley PF (1993) Expression of a mitogen-inducible cyclooxygenase in brain neurons: regulation by synaptic activity and glucocorticoids. Neuron 11: 371–386
28. Zhu Y, Park TS, Gidday JM (1998) Mechanisms of hyperoxia-induced reductions in retinal blood flow in newborn pig. Exp Eye Res 67: 357–369

IV

Josef Krieglstein

Pharmacology of Cerebral Ischemia

1998

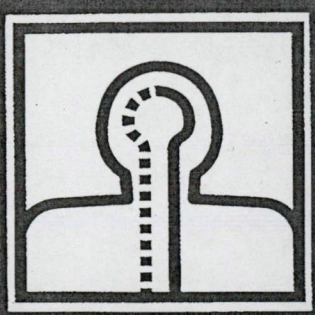

medpharm Scientific Publishers Stuttgart

Pathophysiology of COX-2 and NOS-derived metabolites and free radicals during brain ischemia

D. W. Busija[1], F. Bari[1,2], R. Degi[1,2], F. Domoki[1,2], R. Veltkamp[1], T. M. Louis[3], N. Thrikawala[1], G. Robins[1]

Hypoxia/ischemia is a relatively common occurrence during the perinatal period. After successful resuscitation, an episode of hypoxia/ischemia can be followed by secondary insults. These secondary insults, described in babies as well as experimental animals, include seizure activity, intracranial hemorrhages, edema, secondary release of neurotransmitters such as glutamate, and apnea. It is reasonable to propose that impaired cerebrovascular control mechanisms and inappropriate changes in protein synthesis following the initial insult can predispose the brain to additional damage during these secondary insults.

One important component of the original insult constituting hypoxia/ischemia may be the damage caused by oxygen radicals. We (Armstead et al. 1988; Pourcyrous et al. 1993) and others (Nelson et al. 1992) have shown that the primary source of superoxide anion in the cerebral cortex of piglets and other species is through the metabolism of arachidonic acid by cyclooxgyenase. Superoxide anion is produced on a one-to-one basis with PGH_2, which is an unstable intermediate product that is further metabolized to various prostaglandins and thromboxanes (prostanoids) (Busija 1997). Superoxide anion may act alone, or may combine with nitric oxide (NO) derived from nitric oxide synthase (NOS) to form peroxynitrite (Beckman et al. 1990). Cyclooxygenase can be present as two isoforms (COX-1/-2) (Wu 1996). In apparent contrast to other organs and tissues, the predominant isoform in the cerebral circulation and brain of neonates appears to be COX-2 (Busija et al. 1996a; Peri et al. 1995; Dégi et al. 1998a, b). In the piglet, the constitutive endothelial and neuronal NOS isoforms are located exclusively in vascular and neurons/glial cells, respectively, and the spatial relationship of NOS- and COX-containing cells is consistent with one system affecting the functioning of the other system (Dégi et al. 1998a).

The purpose of our studies was to characterize the role of COX-related mechanisms in mediating short- and long-term changes in cerebrovascular responsiveness relating to the NOS-system following ischemia/reperfusion in piglets. First, we investigated the mechanisms underlying changes in cerebral arteriolar responses to dilator stimuli such as N-methyl-D-

Key words: neonate, ischemia, cyclooxygenase, nitric oxide synthase, cerebral circulation, N- methyl-D-aspartate, oxygen radicals, glutamate receptors.

[1]Department of Physiology and Pharmacology, Wake Forest University School of Medicine, Winston-Salem, NC, USA, 27157; [2]Departments of Physiology and Ophthalmology, Albert Szent-Györgyi Medical University, Szeged, Hungary; and [3]Department of Anatomy and Cell Biology, East Carolina University, Medical School, Greenville, NC, USA, 27858.

J. Krieglstein (Ed.) Pharmacology of Cerebral Ischemia 1998

aspartate (NMDA) that take place after ischemia/reperfusion (I/R). N-methyl-D-aspartate dilates cerebral arterioles via an activation of neuronal NOS and release of NO (Busija and Leffler 1989; Faraci and Breese 1993; Meng et al. 1995). Second, we investigated the role of COX-related mechanisms underlying enhanced protein synthesis after I/R. Specifically, we examined effects of I/R on expression NOS and COX isoforms in cerebral arteries and tissues. We performed these studies in newborn pigs since these animals show similarities in cerebrovascular regulation and state of brain maturation with human babies (Busija 1997).

In experiments using the closed cranial window in piglets, we were the first to demonstrate that NMDA, an analog of glutamate, dilates cerebral arterioles (Busija and Leffler 1989). Glutamate is one of the most prevalent neurotransmitters in the brain. Further, the degree of dilation to NMDA is inhibited by asphxyia (Busija and Meng 1993), ischemia (Busija et al. 1996b), and/or arterial hypoxia (Bari et al. 1998; Veltkamp et al. 1998). Thus, following 10 min of total global ischemia caused by increasing intracranial pressure, arteriolar dilator responses to NMDA are reduced by approximately 50–75% at 1 h after reperfusion, and normal dilator responses return over 2–4 h (Figure 1). The degree of attenuation of dilator responses to NMDA is related to the severity of anoxic stress, such that arterial hypoxia has less of an inhibitory effect while combined hypoxia/ischemia has a greater inhibitor effect. In addition to causing delayed inhibitory effects, NMDA-induced vasodilation is also totally blocked during arterial hypoxia (Bari et al. 1998). In contrast to NMDA, arterial dilator responses to kainate, which are due in part to activation of NOS, are largely unaffected by I/R (Bari et al. 1997a). Since vascular dilator responses to exogenous NO are intact after I/R (Busija et al. 1996b), and because kainate-induced dilation is intact, it seems likely that I/R causes transient dysfunction of the NMDA receptor complex (Hoffman et al. 1994). Inhibition of NMDA-induced dilation may be detrimental to the stressed brain, by disruption of the normal relationship between metabolic rate and blood flow.

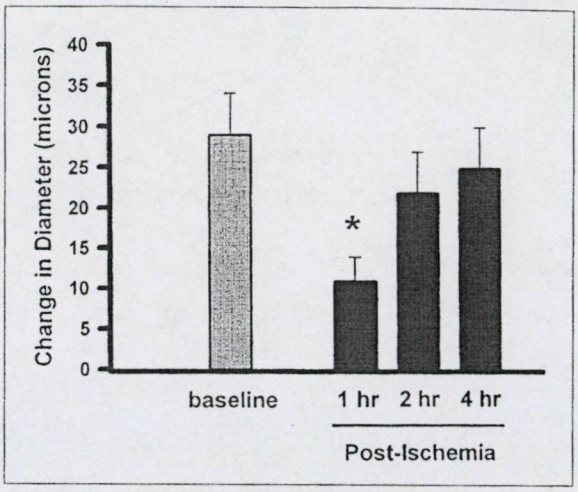

Fig. 1. Absolute change from control arteriolar diameter during application of 10^{-4}M NMDA before (baseline) and after 10 min of ischemia. Ischemia reduced arteriolar dilator responses by over 50% at 1 h. Values are means ± SEM for 6 animals. *$P < 0.05$, compared to baseline response. From Busija et al. 1996.

We have found that several pharmacological approaches which involve inhibition of COX or which involve elimination of specific COX metabolites lead to preserved NMDA-induced dilation. First, intravenous administration of indomethacin, an inhibitor of both COX isoforms, preserves arteriolar dilator responses to NMDA after asphyxia or hypoxia (Busija and Meng 1993; Bari et al. 1998). Second, topical application of superoxide anion by superoxide dismutase to the cortical surface also preserves NMDA-induced dilation (Bari et al. 1998) (Figure 2). The primary source of superoxide anion in the cortex following anoxic stress is from arachidonic acid via the COX pathway (Armstead et al. 1988; Pourcyrous et al. 1993; Nelson et al. 1992). And third, inhibition of protein synthesis with actinomycin D or cycloheximide prevents attenuation of NMDA-induced dilation following I/R (Veltkamp et al. 1998). Cyclooxygenase is a relatively unstable protein that is eventually degraded during metabolism of arachidonic acid, so that protein synthesis is required for continued production of prostanoids. For example, we have shown that prostaglandin synthesis in cultured astroglia is rapidly stopped by protein synthesis inhibitors

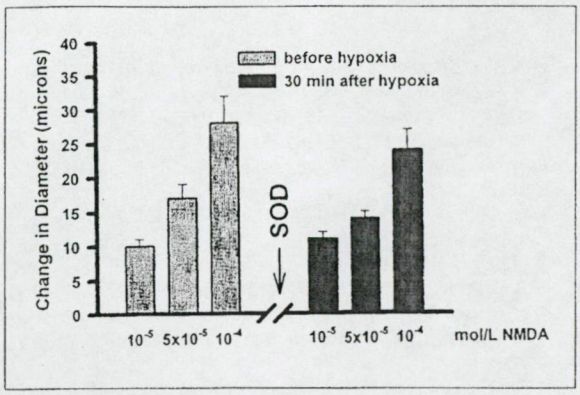

Fig. 2. Absolute change from control arteriolar diameter during application of NMDA before and 30 min following 15 min of exposure to arterial hypoxia in SOD-treated animals (100 U/ml). Treatment with SOD preserved arteriolar dilator responses to NMDA, while dilator reponses after hypoxia in animals not receiving SOD were reduced by greater than 50%. Values are means ± SEM for 6 animals. From Bari et al. 1996.

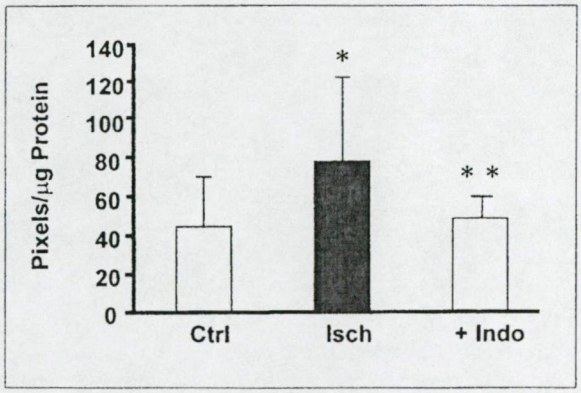

Fig. 3. Histogram of mean pixels per microgram of protein ± SD for eNOS from samples of parietal cortex from time control animals (Ctrl; n= 10), or animals exposed to ischemia (Isch; n=9), or animals exposed to ischemia following indomethacin pretreatment (+ Indo; n=7). Levels of eNOS increased 4–6 h after ischemia, but this increase was prevented by indomethacin pretreatment. *P < 0.05, compared to Ctrl. **P < 0.05, compared to Isch.

(Nam et al. 1995a, b). Thus, COX-dependent processes are involved in the reduction of NMDA-induced arteriolar dilation. In addition, COX-derived superoxide anion may affect arteriolar dilator responses involving endothelium-derived NO (Bari et al. 1997b). In contrast, the involvement of the NO system in attenuating NMDA-dependent dilation is unclear. For example, exogenous NO doesn't affect arteriolar dilator responses to NMDA (Bari et al. 1998).

In addition to having immediate effects, COX-dependent mechanisms may also be involved in more prolonged influences on vascular reactivity by altered protein expression of NOS and COX isoforms after I/R. For example, we have shown that enhanced levels of eNOS but not nNOS occur 4–6 h after I/R, and that this effect is inhibited by indomethacin preadministration (Beasley et al. 1998) (Figure 3). Increases in eNOS were confined to blood vessels. Thus, we would expect that endothelium-dependent response involving NO would be potentiated at this time.

Similarly, levels of COX-2 but not COX-1 increase in cerebral blood vessels and tissues following I/R (Busija et al. 1996a; Dégi 1998a). Levels of mRNA increase rapidly following I/R, and detectible increases in protein levels are present within 2–8 h (Figure 4). In brain cells, the increase in COX-2 mRNA and protein levels are inhibited by indomethacin (Dégi et al. 1998b). However, in blood vessels, indomethacin has little effect on enhanced synthesis of COX-2 (unpublished observations). In addition, inhibition of nNOS by 7-NI has no effect on neuronal expression of COX-2 after I/R (Dégi et al. 1998b), and inhibition of both constitutive NOS isoforms by L-NAME does not alter enhanced COX-2 expression in large cerebral arteries (unpublished observations). Thus, in brain cells but not cerebral arteries, COX-dependent mechanisms are involved in promoting enhanced expression of COX-2. In contrast, inhibition of NOS activity apparently has little effect on COX-2 expression after I/R.

There are several important conclusions and implications from our studies. For example, I/R has diverse yet specific effects on cerebrovascular control mechanisms in the piglet brain. Thus, some but not all dilator responses are impaired after ischemic stress. Failure of normal dilator responses to occur in response to physiological and pathological stimuli during the immediate post-ischemic period may lead to further damage to the cerebral circulation and

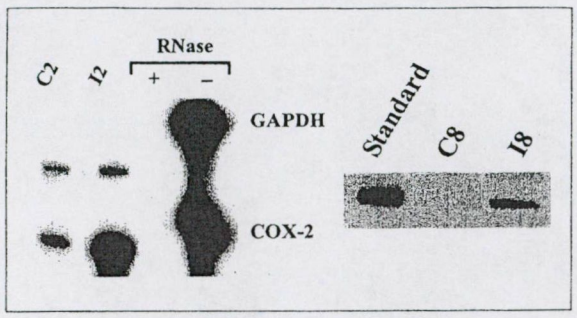

Fig. 4. Effects of ischemia on mRNA (left panel; Rnase protection assay with GAPD representing the housekeeping gene) and protein (right panel; western blot assay) levels for COX-2 in large cerebral arteries. Animals were exposed to 10 min of total global ischemia, and samples were taken at 2 (I2) and 8 (I8) h of recovery. Corresponding time control animals were also done (C2; C8). The mRNA for COX-2 increased at 2 h and the protein level increased by 8 h. In contrast, mRNA for COX-1 did not change after ischemia.

brain. In addition, initial depressor effects on cerebral vasodilator responses are being resolved at a time when enhanced synthesis of eNOS and vascular and neuronal COX-2 is occurring. Since NO and prostanoids are important components of normal cerebrovascular responses to numerous stimuli, responses to these stimuli may be abnormal at a time when secondary insults are known to occur. Further, augmented levels of COX-2 and eNOS may lead to enhanced generation of oxygen radicals during secondary insults, and thus cause greater damage to cells. Thus, possible pharmacological approaches for previously asphyxiated babies could involve inhibition of synthesis or activity of COX.

Acknowledgments

Supported by grants HL-30260, HL-46558, and HL-50587 from the National Institutes of Health, and a grant from the Hungarian Ministry of Education (FKFP 0713/1997).

References

1. Armstead WM, Mirro R, Busija DW, Leffler CW (1988) Postischemic generation of superoxide anion by newborn pig brain. Am J Physiol 255:H401–H403
2. Bari F, Louis TM, Busija DW (1997a) Kainate-induced cerebrovascular dilation is resistant to ischemia in piglets. Stroke 28:1272–1277
3. Bari F, Errico RA, Louis TM, Busija DW (1997b) Influence of hypoxia/ischemia on cerebrovascular responses to oxytocin in piglets. J Vasc Res 34:312–320
4. Bari F, Thore CR, Louis TM, Busija DW (1998) Inhibitory effects of hypoxia and adenosine on N-methyl-D-aspartate-induced pial arteriolar dilation in piglets. Brain Res 780:237–244
5. Beasley TC, Bari F, Thore C, Thrikawala N, Louis T, Busija D (1998) Cerebral ischemia/reperfusion increases endothelial nitric oxide synthase levels by an indomethacin- sensitive mechanism. J Cereb Blood Flow Metabol 18:88–96
6. Beckman JS, Beckman TW, Chen J, Marshall BA (1990) Apparent hydroxyl radical production by peroxynitrite: implications for endothelial injury from nitric oxide and superoxide. Proc Natl Acad Sci USA 87:1620–1624
7. Busija DW (1997) Eicosanoids and cerebrovascular control In: Welch KMA, Caplan LR, Reis DJ, Siesjö BK, Weir B (eds) Primer on Cerebrovascular Diseases. Academic Press, pp 93–96
8. Busija DW, Leffler CW (1989) Dilator effects of amino acid neurotransmitters on piglet pial arterioles. Am J Physiol 257:H1200–H1203
9. Busija DW, Meng W (1993) Altered cerebrovascular responsiveness to N-methyl-D-aspartate after asphyxia in piglets. Am J Physiol 265:H389–H394
10. Busija DW, Thore C, Beasley T, Bari F (1996a) Induction of cyclooxygenase-2 following anoxic stress in piglet cerebral arteries. Microcirculation 3:379–386
11. Busija DW, Meng W, Bari F, McGough PS, Errico RA, Tobin JR, Louis TM (1996b) Effects of ischemia on cerebrovascular responses to N-methyl-D-aspartate in piglets. Am J Physiol 270:H1225–H1230
12. Dégi R, Bari F, Beasley TC, Thrikawala N, Thore C, Louis TM, Busija DW (1998a) Regional distribution of prostaglandin H synthase-2 and neuronal nitric oxide synthase in piglet brain. Pediatr Res 43:683–689
13. Dégi R, Bari F, Thrikawala N, Beasley TC, Thore C, Louis TM, Busija DW (1998b) Effects of anoxic stress on prostaglandin H synthase isoforms in piglet brain. Dev Brain Res 107:265–276
14. Faraci FM, Breese KR (1993) Nitric oxide mediates vasodilation in response to activation to N-methyl-D-aspartate receptors in the brain. Circ Res 72:476–480
15. Hoffman DJ, McGowan JE, Marro PJ, Mishra OP, Delivoria-Papadopoulos M (1994) Hypoxia-induced modification of the N-methyl-D-aspartate receptor in the brain of the newborn piglet. Neurosci Lett 16:156–160
16. Meng W, Tobin JR, Busija DW (1995) Glutamate-induced cerebral vasodilation is mediated by nitric oxide through NMDA receptors. Stroke 26:857–863
17. Nam MJ, Thore C, Busija D (1995a) Rapid induction of prostaglandin synthesis in piglet astroglial cells by interleukin 1α. Brain Res Bull 36:215–218
18. Nam MJ, Thore C, Busija D (1995b) Role of protein synthesis in interleukin 1α-induced prostaglandin production in ovine astroglia. Prost Leuk Ess Fatty Acids 53:69–72
19. Nelson CW, Wei EP, Povlishock JT, Kontos KA, Moskowitz MA (1992) Oxygen radicals in cerebral ischemia. Am J Physiol 263:H1356–H1362

20. Peri KG, Hardy P, Li DY, Varma DR, Chemtob S (1995) *Prostaglandin G/H synthase-2 is a major contributor of brain* prostaglandins in the newborn. J Biol Chem 270:24615–24620
21. Pourcyrous M, Leffler CW, Bada HS, Korones SB, Busija DW (1993) Brain superoxide anion generation in asphyxiated piglets and the effect of indomethacin at therapeutic dose. Pediatr Res 34:366–369
22. Veltkamp R, Domoki F, Louis TM, Busija DW (1998) Inhibitors of protein synthesis preserve the N-methyl-D-aspartate-induced cerebral arteriolar dilation after ischemia in piglets. Stroke, in press
23. Wu, KK (1996) Cyclooxygenase-2 induction: molecular mechanism and pathophysiologic roles. J Lab Clin Med 128:242–245